JULY, 2021 VOL. 2

COUPLING, ENERGETIC AND DYNAMICS OF ATMOSPHERIC REGIONS (CEDAR)

STUDENT NEWSLETTER

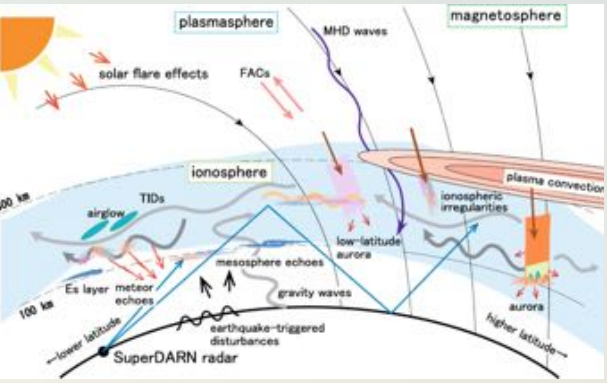

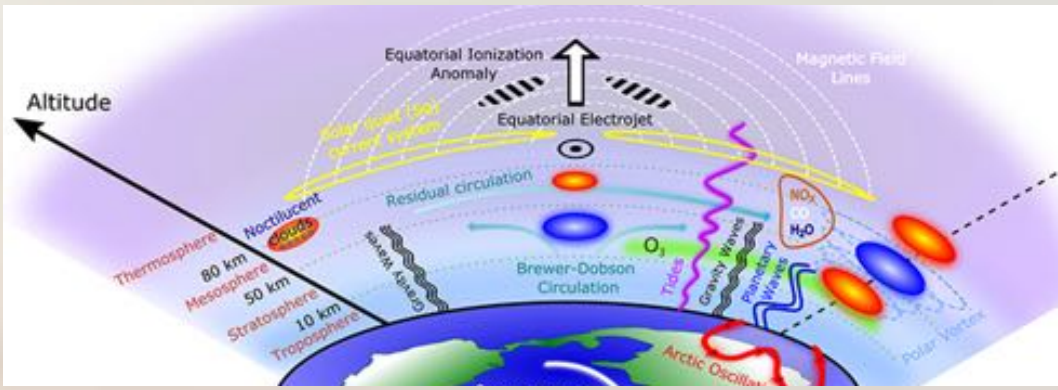

CONTENT

PROLOGUE

2021 CEDAR workshop report*

839 participants registered from 42 countries around the world. The chart below provides the countries and numbers from countries with 5 and more participants.

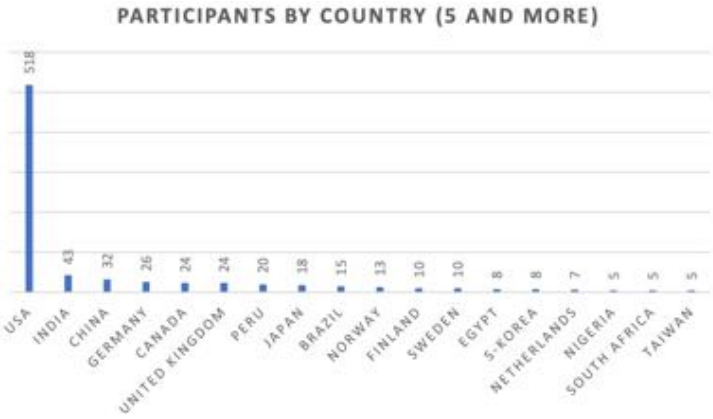

All countries with decreasing participant numbers are: USA, India, China, Germany, Canada, United Kingdom, Peru, Japan, Brazil, Norway, Finland, Sweden, Egypt, S-Korea, Netherlands, Nigeria, South Africa, Taiwan, Argentina, Poland, Puerto Rico, Russia, Turkey, Slovakia, Spain, France, Greece, Iran, Morocco, Singapore, Armenia, Australia, Belgium, Chile, Czech Republic, Ethiopia, Indonesia, Luxembourg, Pakistan, Ukraine, United Arab Emirates, Venezuela. Especially noteworthy is the increased participance from Peru and from African states.

*https://cpaess.ucar.edu/sites/default/files/meetings/2021/documents/cedar_report_2021_07.pdf

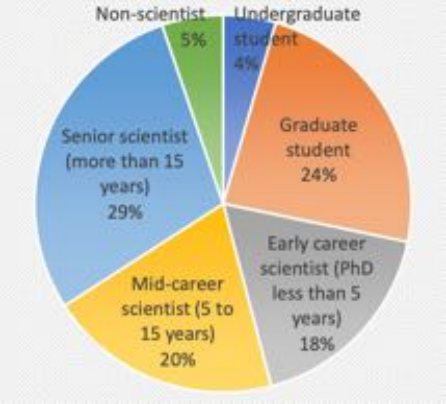

There was an almost even distribution between students, early career, mid-career and senior scientists among the participants. The non-scientist increased compared to last year to 5% (in 2020 it was 3%). From the 38 undergraduates 6 came from Peru, and altogether 11 undergraduates out of 38 were international (29%). There was even a large international participation for graduate students. 105 out of the 199 graduate students came from international institutions (53%) and from 26 countries. The numbers of international participants decrease a bit for early career scientist (45% or 67/148), and stronger decrease for mid-career 37% (63 out of 168), and 25% for senior scientist (60 out of 242). Of the 44 self-identified participants as non-scientist 15 came from international institutions including TMinus Engineering Netherlands, Nammo Raufoss AS Norway, QinetiQ UK; and from the US from National Academy of Sciences, Blue Origin, Virgin Galactic, Computational Physics Inc., Irvington High School, Reeve Engineers. The 518 US participants came from approximately 120 different institutions among them 57 universities and colleges.

STUDENT VOLUNTEERS

Special Thanks!

Deepthi Ayyagari (Indian Institute of Technology Indore, India)

Amadi Brians Chinonso (National Institute for Space Research, Brazil)

Meghan LeMay (Boston University, USA)

Dr. Komal Kumari (Arizona State University, USA)

Onyinye Gift Nwankwo (University of Michigan, USA)

Joaquín Díaz Peña (Boston University, USA)

Andrew Pepper (Clemson University, USA)

Zishun Qiao (Embry-Riddle Aeronautical Univ., USA)

Fan Yang (Embry-Riddle Aeronautical Univ., USA)

INCOHERENT SCATTER RADAR

DR. ASHTON REIMER , SRI
SUMMARY WRITTEN BY ANDREW PEPPER

Credit: UCF Arecibo ISR

Incoherent Scatter Radar is a commonly employed remote sensing technique that utilizes large antenna apertures and megawatt class transmitters to send coded pulses into the earth's atmosphere for a variety of scientific data products. The outputted data products have a direct correlation to the targeted scattering medium which reflects signals back to the receiver for statistical signal processing. From the received signal and eventual processing, physical parameters are inferred from instrument and scattering models with the aid of assumptions. From these data products, physical studies may be conducted on a wide variety of phenomena including (but not limited to): plasma instabilities, ionospheric conductivity, and particle precipitation.

A subtle nuance of any instrument is the fundamental difference between measurements and observations. The foremost is the actual recorded values, which in this case, are represented by voltages turned into lag estimates; whereas the observations are simply the utilization of those measurements to estimate the physical parameter under investigation. In order to accurately derive the observable, a forward model is employed to solve an inverse problem. The forward model (f) contains all of the relevant physics required to predict measurements (y) for a given set

of observations (p), and thus solving the inverse problem may be as simple as solving the left equation in (1). Although, in general practice an extra term is added to the above equation for noise (e) which forces assumptions to be made in order for the right equation to be solved in (1):

$$f^{-1}(y) = p \longrightarrow y = f(p) + e \tag{1}$$

The Radio Detection and Ranging (radar) equation governs the physical limitations of such an instrument by providing the received power (PRx) in relation to properties of the particular system used. Transmitted power (PTx), antenna gain (GTx), effective received area (ARx), loss terms based off the target of measurements (PTx), and the radar cross section of the target (PTx) are used to determine the power of the received signal.

$$P_{Rx} = \frac{P_{Tx}G_{Tx}}{4\pi R_i^2}\sigma\frac{A_{Rx}}{4\pi R_s^2} \tag{2}$$

The distinction between hard and soft targets for radar changes the received signal significantly. For incoherent scatter, the received signal is extremely weak (≈ 10 fW), and is a result of Thomson scattering from the electrons contained in the plasma which acts as a soft target. ISR theory then allows for two limits to be derived; the non-collective limit prevents information on ions from being decoupled from the motion of electrons whereas the collective limit includes an extra factor related to the ion and electron temperatures allowing for the decoupling to occur. ISR theory is then useful for the prediction of statistical properties regarding the power spectrum of the returning scattered signal, and produces range profiles for electron density (Ne), electron and ion temperature (Te/Ti), and line-of-sight velocities (vLOS):

$$\left\langle |\xi_s(\omega)|^2 \right\rangle \overset{\mathcal{F}}{\longleftrightarrow} \langle E_s(t)E_s^*(t-\tau)\rangle \tag{3}$$

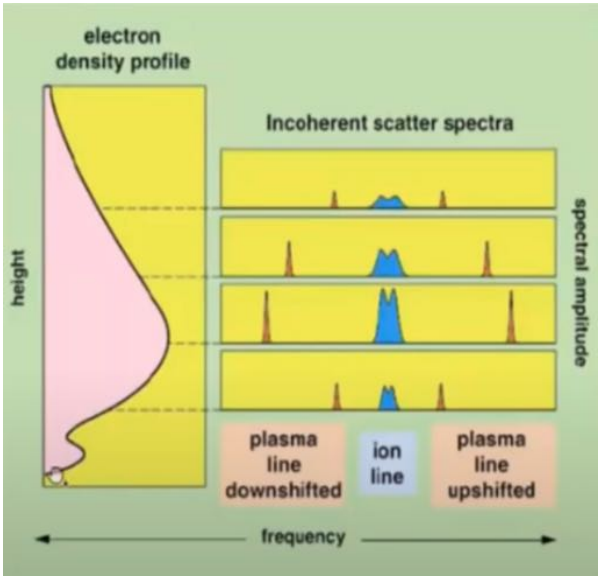

Figure 1. Diagram of ISR detection. Credit Anja Stromme.

An altitude profile for electron density is shown above, and an example of the scattered spectra that could be used to derive the profile is shown on the right. In order to properly predict the right side of equation 3, a forward model is deployed (derived from linear kinetic theory that predicts the power spectrum based off physical parameters) along with a range-lag ambiguity function (direct result of blurring in space and time due to measurement method) to create modeled lag estimates for comparison to the voltage derived lag estimates from the actual measurement. This ensures properly refined data products, and an overview of the process from actual measurements to the outputted information is detailed below.

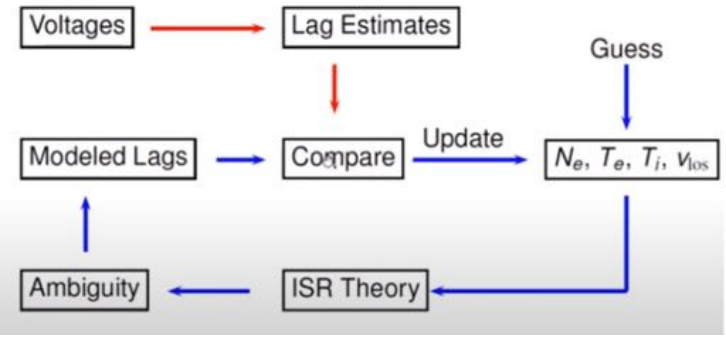

Figure 2. Diagram of ISR detection. Credit Ashton Reimer.

The last element of ISR's to be considered is the assumptions taken during experiments. Any of the four major data products derived from ISRs involve a standard set of assumptions based off either ISR theory or the measurement/ processing dichotomy. Examples of assumptions derived from ISR theory are that particle speeds are Maxwellian distributed or there exists prior knowledge of the plasma composition and collisional rates. When considering measurement and processing assumptions, it is critical to remember that they may slightly vary depending on the actual ISR in question. Generally, plasma parameters are considered to be constant for a typical measurement duration and the range gradients are always greater than or equal to the range resolution of the technique used. Different experiments and facilities have varying assumptions so it is best practice to inquire the respective PI's for more information.

Speaker bio

Dr. Ashton Reimer is a Research Engineer in the Center for Geospace Studies at SRI International in Menlo Park, California. Dr. Reimer earned his PhD in Physics and Engineering Physics at the University of Saskatchewan, Canada in 2018. Beginning in November 2016, Dr. Reimer joined the Advance Modular Incoherent Scatter Radar (better known as AMISR) operations and maintenance team at SRI where to this day he maintains and oversees the data processing, distribution, and archival systems, while supporting other related engineering tasks and user science.

METEOR RADAR

DR. RYAN VOLZ , MIT HAYSTACK OBSERVATORY
SUMMARY WRITTEN BY AMADI BRIANS CHINONSO

INTRODUCTION

RADAR is an acronym for Radio Detection and Ranging, and a detection system that basically uses radio waves to determine range, angle and velocity by measuring the scattering from target objects. Thus, Radars are either coherent or incoherent depending on the scattering they measure, and a typical example of coherent radars is meteor radar. In this tutorial, Dr. Volz explained the principle of operation of meteor radars and their application in atmospheric observations such as measuring wind direction, profiling, temperature, pressure and meteor properties.

Meteor radar is designed to measure scattering from meteor trails and characterized by multiple simple antenna elements, transmitter power of 10s of kilowatts and a fixed operating frequency between the upper HF and lower VHF band (15 – 40 MHz). As the name implies, meteor radars depend on the dynamics of a meteor.

WHAT IS A METEOR?

According to Dr. Volz, small bodies in space, typically less than 1m in diameter and having a speed of about 11 to 72km/s are known as meteoroids. While falling towards the Earth surface, they either burn out as they encounter dense gases or survive passage. Meteoroids that burn out to form plasma or light in the atmosphere (usually at altitudes between 70 to 120 km) are referred to as METEOR while those that survive passage to the earth surface are called METEORITES.

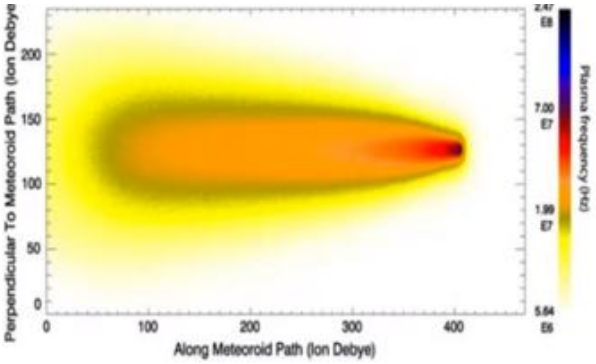

Fig.1: Variation in plasma frequency along the path of the plasma trail. A close look shows that plasma frequency is higher at the plasma head but decreases towards the tail.

Meteors are classified as either shower or sporadic. They are showers if they emanate from a particular parent body such as an asteroid (a larger body than meteorites) or a comet (body of ice, dust and rocks) and their nomenclature depends on the radiant source they appear to emanate from in the celestial frame while sporadics are not known to come from any known showers and usually characterized by location and spatial uniformity. The number of meteor per day varies with time of day with the highest value for meteor count per hour is observed around sunrise and a minimum at sunset which is not unrelated to the Earth's rotation. As at the time of writing this article (09:14 UTC-3), the meteor count for the day was 5495 and still counting (https://ccar.colorado.edu/meteors/). This implies a continuous change in the density of background plasma and can be used as a yardstick to measure direction and profile of wind and other atmospheric characteristics.

WORKING PRINCIPLE OF METEOR RADAR

The previous section makes clear that meteors appear in the atmosphere all through the day, though at varying rate. Dr. Volz explained that the plasma trail formed by meteors, coherently reflect scattered incident signals and the relationship between the incident and scattered wave vector, known as the Bragg vector is given as shown in equation 1.

$$\vec{k}_B = \vec{k}_s - \vec{k}_i \ldots\ldots\ldots 1$$

Additionally, the plasma trails are characterized by alternating Fresnel zones of constructive and destructive interference as shown in figure 2, with primary reflected signal contributions coming from the first Fresnel zone given by equation 2.

$$d_f = \sqrt{2d\lambda} \ldots\ldots\ldots 2$$

The reflected signal (echo) is said to be underdense when the plasma frequency is much less than the radar frequency or overdense for conditions where the plasma frequency is much greater than the radar frequency. Overdense conditions cause the plasma trail to act as a reflecting surface and avoid the radar signal from permeating into the plasma. This is known as the Ceiling effect. Thus, radar frequency must be within a range which will permit enough entrance into the meteor trail and reduce ionospheric effects. This is why radar signals have frequency between 15 and 40 MHz (HF/VHF frequencies) and most detection are observed between 80 and 100 km altitude.

To locate meteors at the aforementioned altitude, signals are sent and subsequently received by array of antennas (Dipole or Yagi) that provide two angular estimates

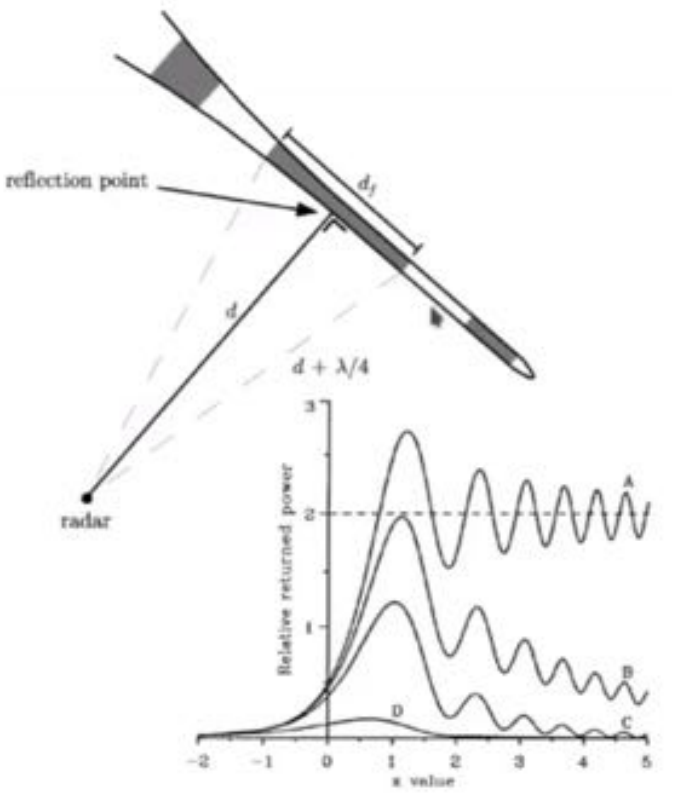

Fig.2: a) Plasma trail with alternating Fresnel zones of constructive and destructive interference. The first Fresnel zone with df is constructive and represented by first section on the plot. b) The plot shows the alternating regions of constructive and destructive interference as well as a consistent decline in return power due to decrease in plasma frequency along the trail.

as shown in figure 3 and related to the phase difference by equation 3.

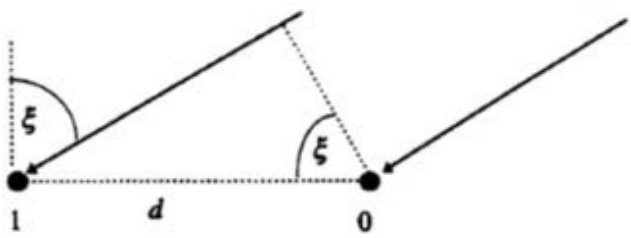

Fig.3: Two angular estimates from an array of antenna used to estimate phase difference.

$$\emptyset_{10} = -2\pi \frac{d}{\lambda} sin\xi \ldots\ldots\ldots 3$$

Where $\emptyset_{10}$ is the phase difference.

MEASURING WIND DIRECTIONS

Dr. Volz further explained that the direction of drift of plasma trail is in the direction of neutral wind and thus, introduces Doppler frequency shift into the Bragg vector direction and related as follows:

$$f_D(x,y,z,t) = \frac{1}{2\pi}\begin{bmatrix} k_x & k_y & k_z \end{bmatrix}\begin{bmatrix} u(x,y,z,t) \\ v(x,y,z,t) \\ w(x,y,z,t) \end{bmatrix} \ldots\ldots 4$$

Where, $kx\ ky\ kz$ are the Bragg vector components while u, v, w are the unknown wind components. These components can be obtained by solving several set of equations within a given volume as shown in figure 4.

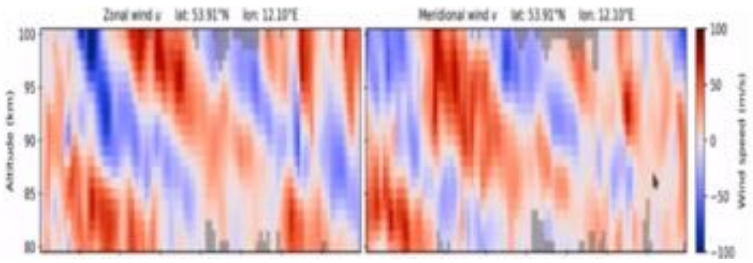

Fig.4: The zonal and meridional wind velocities. This is usually obtained from the Doppler shift introduced into Bragg's vector by the wind.

MEASURING TEMPERATURE AND PRESSURE

In addition to measuring wind, meteor radar can be used to measure temperature and pressure. Dr. Volz explains that since the ambipolar diffusion coefficient D_a can be related to the exponential decay of the echoes power, which in turn is a function of the plasma trail radius, it is then possible to obtain temperature and pressure since they relate with D_a as given in equation 5.

$$D_a \propto \frac{T^2}{P} \ldots\ldots\ldots 5$$

Furthermore, meteor radars can estimate the mass flux from meteoroids, meteoroid orbit, populations and also study meteor plasma dynamics and instabilities such as Sporadic E layers.

FUTURE OF METEOR RADAR

Dr. Volz presented an innovative meteor radar network consisting of transmitters with unique pseudorandom codes with adjacent receivers able to decode signals from several transmitters similar to the GNSS systems as shown in figure 5.

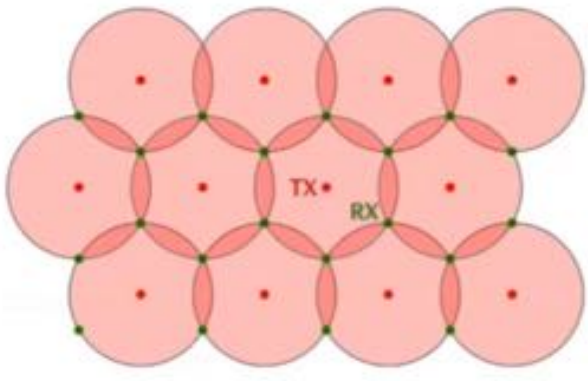

Fig.5: Meteor radar network consisting of transmitters and receivers. These transmitters have unique codes that allow each receiver to decode and trace signals from each transmitter.

Unlike a single meteor radar that averages over the space under study, this network system provides a possible platform for more, and accurate detections in a sample space and can as well estimate the 3-D wind field as a function of time as shown in figure 6.

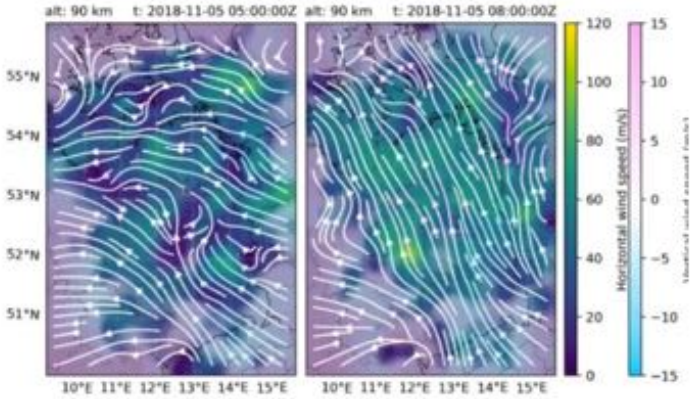

Fig.6: 3-D wind field as a function of time, made possible by network of meteor radar.

CONCLUSION

Meteor radar estimates wind velocity by measuring the Doppler shift of the received signal after scattering incident waves by the meteor trail at about 80 to 100 km. Meteor radar has several strengths and they include continuous operation, good spatial coverage even in the midst of overlapping networks and relatively less expensive to build.

Speaker bio

Dr. Ryan Volz is a Research Scientist at MIT Haystack Observatory with interests in signal processing, statistical estimation, and novel instrumentation applied particularly to radio science. He and colleagues at CU Boulder are currently developing the Zephyr meteor radar network, a novel multiple-input/multiple-output (MIMO) system designed to estimate the 3-D wind field in the upper atmosphere by way of meteor trail scattering.

SOUNDING ROCKET MEASUREMENTS WITH VAPOR TRACES AND THE TRIANGULATION TECHNIQUE

DR. RAFAEL MESQUITA , CLEMSON UNIVERSITY
SUMMARY WRITTEN BY ANDREW PEPPER

Fig.1. TMA Trail evolution (photo credits: Rafael Mesquita)

Sounding rocket campaigns have historically been deployed at various rocket ranges as a method for validating ground and satellite based measurements. Besides being inexpensive when compared to other instruments (ISR and satellites), sounding rockets allow for critical in-situ measurements to be taken at altitude ranges where snapshots of small-scale atmospheric dynamics can be difficult to measure otherwise. Sounding rockets are often classified as a high-risk experiment due to their success rate, limited number of launch sites, and requirement of clear nights when triangulation is considered.

Vapor traces, such as trimethylaluminum (TMA) , are able to stay cost effective to deploy on sounding rocket campaigns thanks to only requiring mechanical systems as opposed to sophisticated electronic components. Because of this, chemical release techniques remain widely utilized to study neutral winds in the upper atmosphere while providing generally low magnitude error bars.

The procedure of triangulation is fairly simple; once the rocket is at the pre-determined altitude, the chemical tracer begins to be released. Photographs tracking the evolution of the tracer are taken from multiple locations on the ground at regular intervals. An example of this is provided in Figure 1.

With the pointing angles of the cameras and known location of the camera sites, the original photo pairs may be converted to astronomical coordinates (right ascension and declination) which provide three dimensional locations of the target (tracer). A brief diagram displaying the relationship between camera site, pointing angles, and the tracer is displayed in the Figure 2.

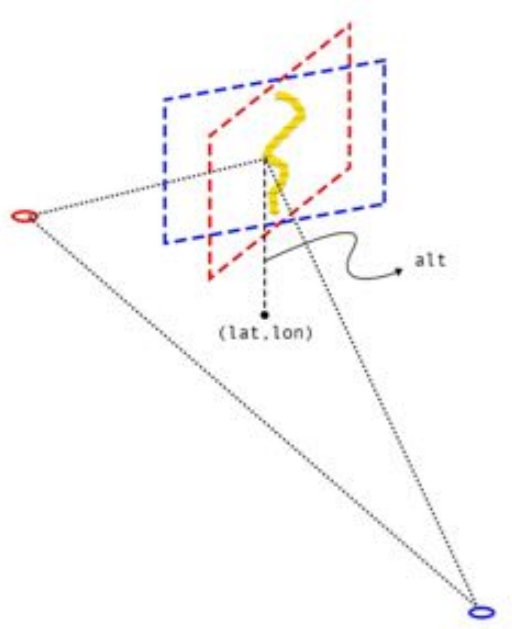

Fig.2. Diagram displaying the relationship between camera site, pointing angles, and the tracer.

The triangulation technique then provides a set of positions changing with respect to time which allows us to produce a linear fit for estimating the wind profiles as described by the following equations:

$$u = r\cos\theta\frac{d\phi}{dt}$$

$$v = r\frac{d\theta}{dt}$$

The above equations are for the zonal and meridional winds respectively. In order to obtain the error derived from the triangulation process, the distance of closest approach between the projections (line of sights from the camera sites) is used to weight the fitting of the positions. More confidence in the positions inevitably leads to better fitting, and this in turn minimizes the errors which are derived from the diagonal components of the covariance matrix. This technique can yield errors ranging from roughly 3-5 m/s for a given triangulation process, but this is subject to a variety of conditions. The process from tracer images to velocity profiles of winds is lengthy, but the usefulness of the scientific data outputs keeps sounding rocket campaigns a popular choice for measuring winds in the atmosphere between 80-200 km.

Chemical tracers are but one option of instrumentation deployable via sounding rockets. In situ measurements using a variety of payload components are used to measure aspects of the atmosphere like

electric and magnetic fields, as well as ion and electron temperatures. There exists an abundance of informational material covering these other methods from either NASA Wallops or past CEDAR presentations.

Speaker bio

Dr. Rafael Mesquita earned his PhD in Physics from Clemson University in May 2021. He will start his post-doc at Johns Hopkins University Applied Physics Laboratory in early July. Dr. Mesquita's research interests are mid- and high-latitude neutral dynamics and magnetosphere/ionosphere/thermosphere coupling. His research includes the study of instabilities in the lower thermosphere and auroral forcing using sounding rockets. Dr. Mesquita is an experimentalist who spent much of his PhD analyzing sounding rocket data to produce winds and position of atmospheric instabilities through the triangulation technique and the release of vapor tracers.

OPTICAL INSTRUMENTS

Dr. ASTI BHATT, SRI
SUMMARY WRITTEN BY FAN YANG

Basics of optical emissions in the upper atmosphere:

The dominant emissions is due to dissociative recombination and particle impact excitation. They are both fast process to create photons. They are responsible for airglow, and aurora, respectively.

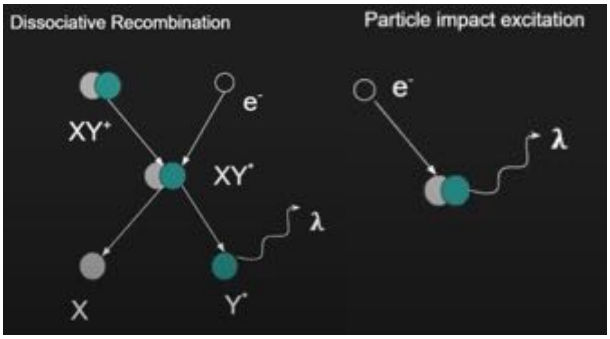

Fig. 1. Emission mechanics. Left: dissociative recombination. Right: particle impact excitation.

All-sky camera with a fisheye lens is commonly used. With the help of different filters, images of different frequency ranges can be captured. It's hard to tell the physical process by the images themselves thus a few methods have been used to make senses of all-sky images. The first way is that the images will project on a map or a grid. Here shows an example in Fig2. Difference between consecutive images can help enhance weak features. Another way is keograms. There may be multiple propagation directions in one image. Keograms allow us to identify individual propagating features. These 2 methods can be both used to study airglow and aurora observed by all-sky imagers.

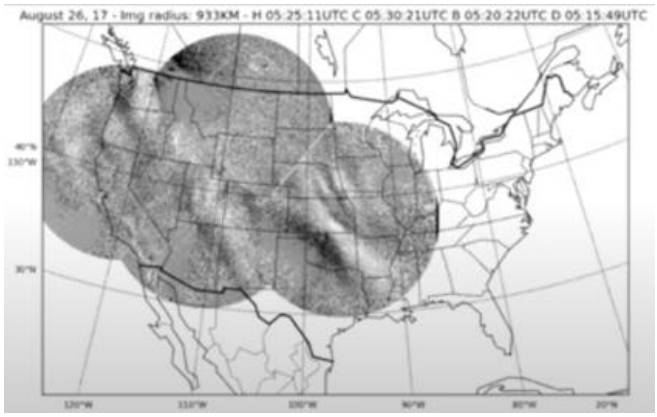

Fig.2. Map of multiple all-sky images.

Fabry-Perot Interferometer [FPI] can be used to measure neutral wind and temperature. Fig3 shows a measurements of wind by multiple FPI at different locations over Alaska.

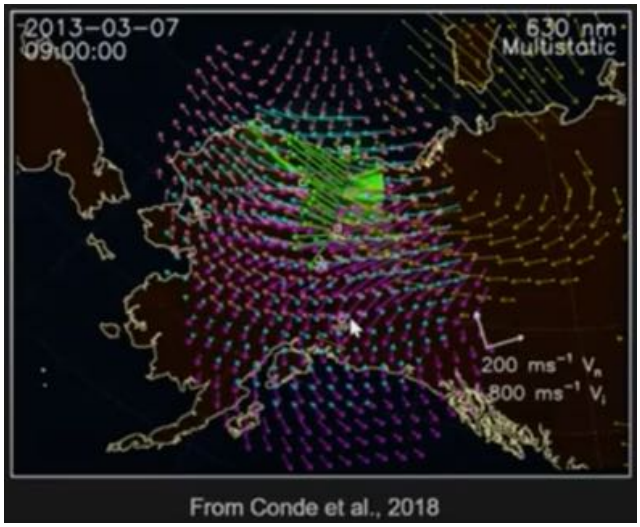

Fig.3. Neutral wind vectors from multiple FPI over Alaska.

Trick things in Optical observation:
limited by weather and location, mounting and enclosure can also effect the observation. Ambient light is another thing to keep in mind. Also, there are a lot of data to process every night.

Speaker bio

Dr. Asti Bhatt has over 10 years of experience as an ionospheric scientist. She currently leads two active NSF projects. On the DASI MANGO project, she builds, installs, and calibrates optical imagers to create a nested network of red and green line optical imagers. She also develops data management and analysis systems, and mentors students. On the Integrated Geoscience Observatory, supported by NSF EarthCube and Cyberinfrastructure for Sustained Scientific Innovation awards, she has led a team to build a software platform designed to increase collaboration among geoscientists and ensure scientific reproducibility, and led community discussion on data and software stewardship. For these projects, Dr. Bhatt manages a team of early- and mid-career scientists and interfaces with partners from collaborator institutions. She has chaired several national and international academic conference sessions at AGU, COSPAR, and CEDAR meetings, and serves on science steering committees for CEDAR, COSPAR Commission C, and Radio Frequency Ionospheric Interactions Workshops.

Small Satellites

DR. JONATHON BRENT PERHAM, MIT LINCOLN LAB
SUMMARY WRITTEN BY DR. KOMAL KUMARI

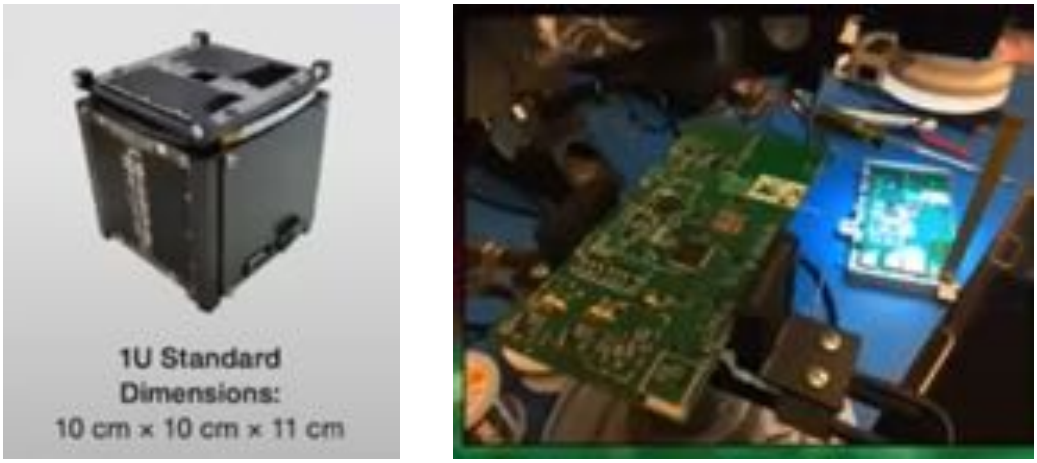

Figure: (Left) a CubeSat and (right) an example of inside circuit design in a CubeSat.

Small satellites such as CubeSats are being popular because of their small size and the ability to collect data at small cost. CubeSats are typically shaped as cube and the different cubes can be attached together to increase the size of the whole satellite. Dr. Perham compared the size of a CubeSat with a cell phone device. The size of a typical CubeSat is 10 cm X 10 cm X 11 cm and it can weigh up to few kilograms.

The inside of a CubeSat contains a circuit which looks like a circuit design of a cellphone device. CubeSats have their own radio transmitter, power, propulsion, sensors and payload. It can be attached to whatever is going into space and it does not require primary and secondary instruments to carry it to space. It can be ejected in space during launch, so any launch provider such as SpaceX and different rocket labs can carry these small satellites. One can put several CubeSats where we don't have any observational capacity and sample data to explore science. Such as Mars cube one (Marco) launched by JPL, NASA which had been flown to Mars.

CubeSats is like a system integration problem so that the whole system is tightly working together to provide useful in situ observational data. The payload has to be appropriately small enough to fit in CubeSat. In order to operate the satellite, one needs to have appropriate software. Once it is launched into space, one needs to do the attitude control with the software as well as protect it from heat and radiation in space. CubeSats needs not only good software but also proper testing.

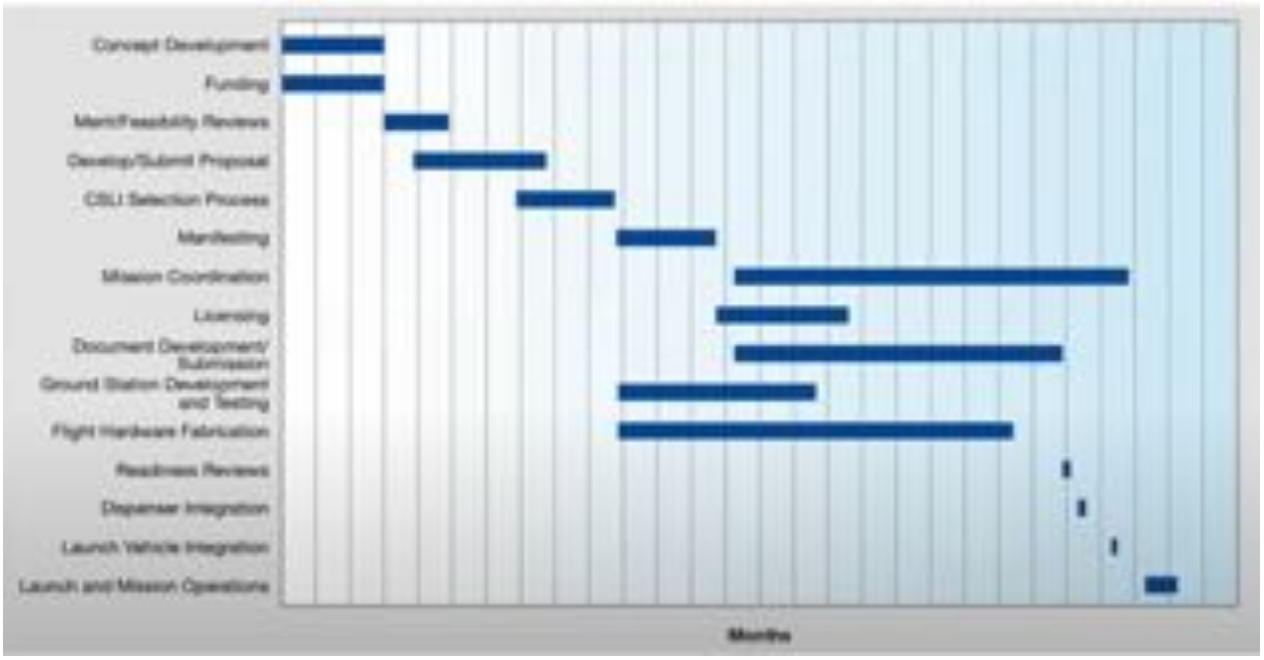

Figure: The flow chart of a CubeSat mission

The above flow chart shows the extensive process from designing the CubeSats to launching them.

Dr. Perham talked about the journey of his own CubeSat mission Andesite. Andesite satellite, launched in June 2020, had 6 small satellites and each of them had a magnetometer and GPS. It was being flown in auroral zone to measure the current system.

Figure: Andesite with six small satellites

From the mission experience, the following key points were listed by Dr. Perham which are necessary to consider when one plans to work on a CubeSat mission.

1. One should not underestimate the importance of a robust flight software on a satellite to get it to work.

2. One should rigorously stress over what may happen when the satellite is in orbit. There is no way to fix hardware once it is up into space.

3. One must be ready with their instrument before the launch provider decides to fly. This provides additional time to do testing.

Speaker bio

Dr. J. Brent Parham is a member of the Technical Staff in the Space Systems Analysis and Test Group at MIT Lincoln Laboratory, where he has studied the space environment and its effects on national infrastructure for the past ten years. Before joining the group, Dr. Parham received a bachelor's degree in Aerospace Engineering from MIT. During his time employed at Lincoln Laboratory he earned a master's in Mechanical Engineering, and a doctorate in Electrical Engineering from Boston University as part of its Center for Space Physics. He has been involved with several cubesat build efforts over the years, including BU's ANDESITE mission that was launched in 2020, and is currently supporting several missions to develop next generation space weather instruments.

THE HITCHHIKER'S GUIDE TO GNSS

DR. SEEBANY DATTA-BARUA, ILLINOIS INSTITUTE OF TECHNOLOGY .
SUMMARY WRITTEN BY AMADI BRIANS CHINONSO

INTRODUCTION

Dr. Datta-Barua's tutorial entailed the basic principles of Global Navigation Satellite System (GNSS), the effect of the ionosphere on GNSS signal propagation and the sensing (study) of the ionosphere using errors introduced by same. The ionosphere is a region of the atmosphere extending from an altitude of about 50 to 1000km and characterized by sufficient amount of electrons to affect radio wave propagation (including GNSS). Typically, GNSS consists of space, user and ground segments with the space segment consisting of a constellation of satellites while the user segments include receivers for positioning, navigating and timing. The ground segment consists of control stations and antenna systems from which operators maintain the satellite constellation. Since GNSS are passive one-way downlink systems, signals are transmitted from satellites to receivers on earth.

To use these signals for positioning, the user's receiver computes the time interval Δt between transmission (from the satellite) and receipt (at the receiver), and by multiplying with the speed of light, the distance r1 of the receiver from the satellite is obtained. That is,

$$r_1 = c\Delta t_1$$

Similar calculations from n number of satellites can give multiple distances $r1, r2, \ldots, rn$ and this gives the position of a receiver in n-1 dimensions because an unknown receiver clock bias must also be solved. Hence, for a three dimensional position, four satellites are required.

THE IONOSPHERE IS REFRACTIVE

Between the satellite and the receiver is a refractive region known as the ionosphere formed as a result of the ionizing property of solar radiation or energetic particles, where the signal becomes delayed owing to decrease in speed of the signal and a subsequent increase in group refractive index (n > 1). Thus, the ionospheric delay is a function of the increase in refractive index given as:

$$n \approx 1 + \frac{X}{2} \ldots\ldots\ldots\ldots\ldots 1$$

Where X is a function of the electron content of the ionosphere given as:

$$X = \frac{f_{pe}^2}{f^2} \propto \frac{N_e}{f^2} \ldots\ldots\ldots\ldots\ldots 2$$

Where f_{pe}^2, f^2 and N are plasma electron frequency, signal frequency and electron density respectively. This implies that the distance measured by the receiver will be longer than normal and as such, introduces an error known as range error. According to Dr. Datta-Barua, range error is proportional to the integrated electron density along the signal path. That is,

$$I = \int (n-1)\, dl = \frac{40.3}{f^2} \int N_e dl = \frac{40.3}{f^2} TEC \ldots\ldots\ldots 3$$

where Eq. (3) gives range error in units of meters. Thus, the ionosphere introduces a significant amount of error in positioning, navigation and timing using GNSS especially for single frequency receivers. However, by using a dual- frequency receiver, range error can be eliminated by using the method of differencing. Additionally, since these errors depend on the plasma properties (refraction and diffraction) of the ionosphere, they can be used as yardsticks to sense (study) the ionosphere.

GPS OUTPUT, TEC AND SCINTILLATIONS

Several types of GNSS are used all over the world and these include GPS, Galileo, GLONASS, Beidou, etc. However, for the purpose of this tutorial, Dr. Datta-Barua explained the structure of the GPS signal and output. A typical GPS signal consists of data of a fixed bit rate overlaid on the coarse acquisition (C/A) code with a characteristic Pseudo-range number (PRN) peculiar for each satellite. Data carries information about the satellites' position, health, etc. However, propagating from satellite to receiver on earth requires a lot of power and as such, a carrier wave, sinusoidal in shape and produced by oscillating atomic clocks, is used to convey the data-code signal. Binary Phase Shift Keying (BPSK) is the modulation method by which a carrier wave's phase changes as the binary numbers (0s and 1s) of the data and C/A code flip as shown in figure 1. The signal received by the receiver antenna is basically the BPSK modulated L1 carrier.

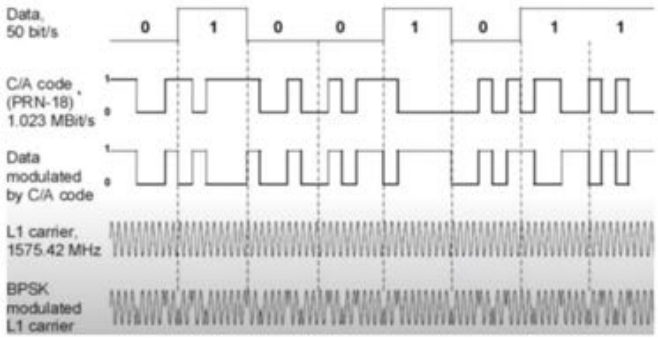

Fig.1. Signal structure of GPS (Dr Seebany, CEDAR-2021).

With the aforementioned inputs, a GPS is able to pre-process the signal, acquire satellites, track satellites and give out the pseudo-ranges (ϱ) (noisy) and carrier phases (φ) (less noisy but have an ambiguous estimate of number of cycles (N) as shown in figure 2.

$$\rho_1 = r + I_s + \varepsilon_{\rho 1}, \quad \text{where } I_s \propto \frac{TEC}{f_1^2}$$

$$\rho_2 = r + \gamma\left(I_s + IFB + \tau_{gd}\right) + \varepsilon_{\rho 2}$$

$$\phi_1 = r - I_s + N_1\lambda_1 + \varepsilon_{\phi 1}$$

$$\phi_2 = r - \gamma\left(I_s - IFB - \tau_{gd}\right) + N_2\lambda_2 + \varepsilon_{\phi 2}$$

$$\gamma = \frac{f_1^2}{f_2^2}$$

Fig.2. Typical GNSS output showing pseudo-ranges and carrier phases (Dr. Datta-Barua, CEDAR-2021).

From figure 2, it is easy to see that the total electron content (TEC) of the ionosphere can be obtained from the slant range error (Is). This is known as the slant TEC.

However, slant TEC is converted to its equivalent vertical TEC by a factor dependent on the elevation angle as shown in equation 4 for a flat earth. However, other researchers including Dr. Datta-Barua uses equation 5 for this conversion. With the vertical TEC, a map can be plotted with the Ionospheric Piercing Point (IPP≈350-400km) as the reference height. The unit of TEC is denoted as TECU and 1 TECU = 10^{16} electrons/m^2

$$vTEC(t) \cong STEC(t) * secZ \ldots\ldots 4$$

$$vTEC(t) = \frac{STEC}{M(el)} \ldots\ldots 5$$

where

$$M(el) = \frac{1}{\cos\left(\arcsin\left(\frac{R_e \cos(el)}{R_e + h_{iono}}\right)\right)}$$

$$Z = zenith\ angle$$

$$R_e = radius\ of\ the\ earth$$

$$h_{iono} = height\ og\ ionospheric\ shell$$

A plot of VTEC against longitude and latitude gives a map known as a TEC map.

GNSS signals can also give information about scintillations in the ionosphere. Scintillations are fluctuations in amplitude and/or phase of GNSS signals due to scattering by plasma irregularities.

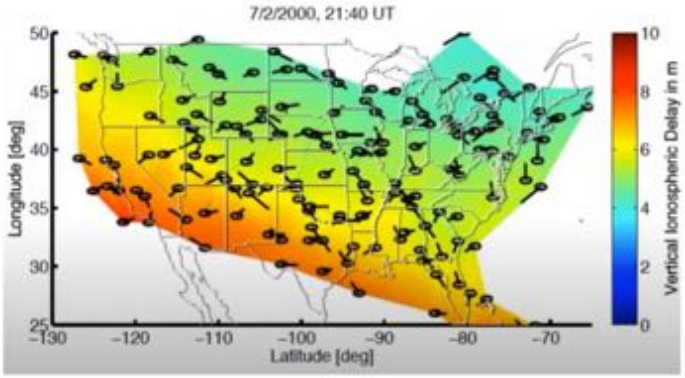

Fig. 3. TEC MAP- A map of VTEC plotted against longitude and latitude, in units of meters at L1 frequency. Note that here 1 m of ranging error = 6.13 TEC units.

Scintillations can lead to loss of lock or tracking experienced by users of certain receivers during disturbed ionospheric conditions. Specialized receivers are typically required to study scintillations; however, a standard dual-frequency receiver can be used to measure scintillations by computing the rate of change of TEC (ROT).

CONCLUSION

The ionosphere plays a vital role in radio wave communication. However, it can be a source of error for transionospheric radio-navigation signals such as GNSS. The error due to the ionosphere varies with the electron density or TEC, thus, this can be used as a yardstick to sense the ionosphere as already described. Students can obtain TEC data from the madrigal website http://millstonehill.haystack.mit.edu/.

Speaker bio

Dr. Seebany Datta-Barua is an Associate Professor of Mechanical and Aerospace Engineering at Illinois Institute of Technology in Chicago, Illinois, USA. Prof. Datta-Barua researches: the use of Global Navigation SatelliteSystems (GNSS) for remotely sensing the atmosphere and Earth's surface; tomography and data assimilation for ionospheric and thermospheric prediction of dynamics; and upper atmospheric effects on GPS-based navigation systems. Dr. Datta-Barua has received the NSF CAREER award and, in 2019, the Institute of Navigation's Per Enge Early Achievement Award for "outstanding contributions to the understanding of the dynamics of the ionosphere and its impacts on satellite-based navigation integrity."

SATELLITES: PAST PRESENT AND FUTURE

DR. KATELYNN GREER , CU-LASP
SUMMARY WRITTEN BY DEEPTHI AYYAGARI

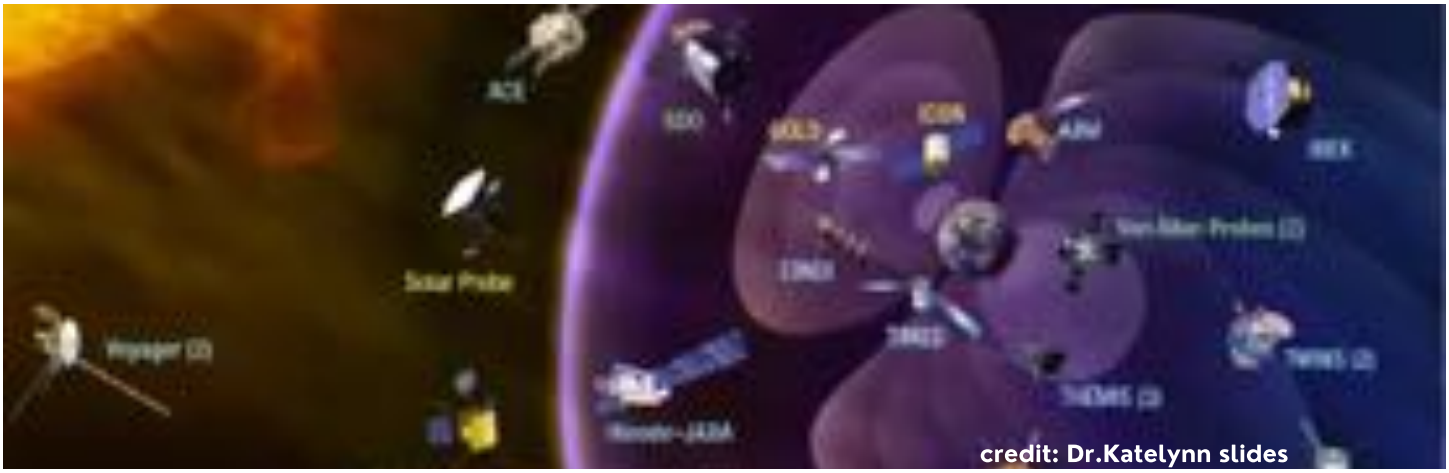

As a matter of fact, we are well aware that a satellite is a moon/object that orbits a planet or star. For example, Earth is a satellite because it orbits the sun. Likewise, the moon is a satellite because it orbits Earth. Usually, in the context of spaceflight "satellite" refers to a machine that is launched into space and moves around Earth or another body in space. The bird's-eye view that satellites have allows them to see large areas of Earth at one time. This enables satellites to quickly collect more data compared with ground-based instruments. Sputnik 1 was the first satellite in space. The Soviet Union launched it in 1957.

Fig. 1. Various spaceflight satellite missions

NASA has launched dozens of satellites into space, starting with the Explorer 1 satellite in 1958. Explorer 1 was US's first man-made satellite. The main instrument aboard was a sensor that measured high-energy particles in space called cosmic rays. The first satellite picture of Earth came from NASA's Explorer 6 in 1959. TIROS-1 followed in 1960 with the first TV picture of Earth from space.

NASA missions: How and Why?

Decadal Survey

- These missions provide an overview of the science and a broad survey of the current state of knowledge in the field.
- Identify the compelling science challenges considering scientific value, urgency, cost category, and risk.
- To develop an integrated research strategy that will present means to address these targets.

Experiment Name	Spacecraft Name	Principal Investigator
Atmospheric Density Accelerometer (MESA)	AE-C	Champion, Kenneth
Bennett Ion-Mass Spectrometer (BIMS)	AE-C	Brinton, Henry
Capacitance Manometer	AE-C	Rice, Carl
Closed-Source Neutral Mass Spectrometer	AE-C	Pelz, D.
Cold Cathode Ion Gauge	AE-C	Rice, Carl
Cylindrical Electrostatic Probes (CEP)	AE-C	Brace, Larry
Extreme Solar UV Monitor (ESUM)	AE-C	Heath, Donald
Low-Energy Electrons (LEE)	AE-C	Hoffman, Robert
Magnetic Ion-Mass Spectrometer (MIMS)	AE-C	Hoffman, John
Magnetometer (Spacecraft)	AE-C	Zmuda, Alfred
Neutral Atmosphere Temperature (NATE)	AE-C	Spencer, Nelson
Open-Source Neutral Mass Spectrometer	AE-C	Nier, Alfred
Photoelectron Spectrometer (PES)	AE-C	Doering, John
Retarding Potential Analyser/Drift Meter (RPA)	AE-C	Hanson, William
Solar EUV Spectrophotometer (EUVS)	AE-C	Hinteregger, Hans
Temperature Alarm	AE-C	Caruso, Paul
Ultraviolet Nitric-Oxide (UVNO)	AE-C	Barth, Charles
Visible Airglow Photometer (VAE)	AE-C	Hays, Paul

Experiment Name	Spacecraft
Auroral Physics Theory	Dynamics Explorer 1
Controlled and Naturally Occurring Wave Particle Interactions Theory	Dynamics Explorer 1
Energetic Ion Composition Spectrometer (EICS)	Dynamics Explorer 1
High Altitude Plasma Instrument (HAPI)	Dynamics Explorer 1
Magnetic Field Observations Triaxial Fluxgate Magnetometer (MAG-A)	Dynamics Explorer 1
Plasma Waves Instrument (PWI)	Dynamics Explorer 1
Retarding Ion Mass Spectrometer (RIMS)	Dynamics Explorer 1
Spin Scan Auroral Imager (SAI)	Dynamics Explorer 1

ACE - operational since 1998
TIMED - operational since 2002

These early missions have an intense impact on today's science.

- GOLD
- ICON

"The tables here in this page give us all the historical highlights of heliophysical missions"

Experiment Name	Spacecraft
Atmospheric Dynamics and Energetics Investigation	Dynamics Explorer 2
Fabry-Perot Interferometer (FPI)	Dynamics Explorer 2
Ion Drift Meter (IDM)	Dynamics Explorer 2
Langmuir Probe (LANG)	Dynamics Explorer 2
Low Altitude Plasma Instrument (LAPI)	Dynamics Explorer 2
Low Altitude Plasma Investigation High Angular Resolution	Dynamics Explorer 2
Magnetic Field Observations (MAG-B)	Dynamics Explorer 2
Magnetospheric Energy Coupling To The Atmosphere Investigation	Dynamics Explorer 2
Neutral Atmosphere Composition Spectrometer (NACS)	Dynamics Explorer 2
Neutral-Plasma Interactions Investigation	Dynamics Explorer 2
Retarding Potential Analyzer (RPA)	Dynamics Explorer 2
Vector Electric Field Instrument (VEFI)	Dynamics Explorer 2
Wind and Temperature Spectrometer (WATS)	Dynamics Explorer 2

Future Satellite Missions

Major focus is on the research missions like **Geospace Dynamics Constellation**. A mission designed with constellation of 6 satellites

- Understand how the high latitude ionosphere and thermosphere system responds to variable solar wind/magnetosphere forcing.

- Understand how internal processes in the global ionosphere -- thermosphere system redistribute mass, momentum and energy.

Few more missions are shown below:

AWE
Atmospheric Waves Experiment
- 2022-ish
- ISS

TRACERS
- Tandem Reconnection and Cusp Electrodynamics Reconnaissance Satellites
- No earlier than August 2022

SunRISE
- Sun Radio Interferometer Space Experiment
- 6 cubesats
- Solar particle storms
- No earlier than July 2023

Tips Tricks & Pitfalls

- Use Quality Flags.
- Keep track of Local Time.
- Acknowledging data from authentic pages is mandatory: publications, projects etc..
- It's equally important to (i) create a science team, (ii) propose a mission and build a team for it.

Speaker bio

Dr. Katelynn "Katie" Greer studies the thermosphere and its connection with the ionosphere and lower atmosphere. She is particularly interested in quiet geomagnetic conditions, longitudinal variability, and local time structures. She has also been working on developing FUV hardware instrumentation. She received her PhD in Aerospace Engineering Sciences from the University of Colorado Boulder in 2013 and completed a post-doc at the University of California – Berkeley where she worked on the ICON mission. She has been with LASP since 2017. In 2020, she was awarded the NASA Early Career Public Achievement Medal.

HIERARCHY OF ATMOSPHERIC MODELS

DR. XIAN LU , CLEMSON UNIVERSITY
SUMMARY WRITTEN BY ONYINYE GIFT NWANKWO

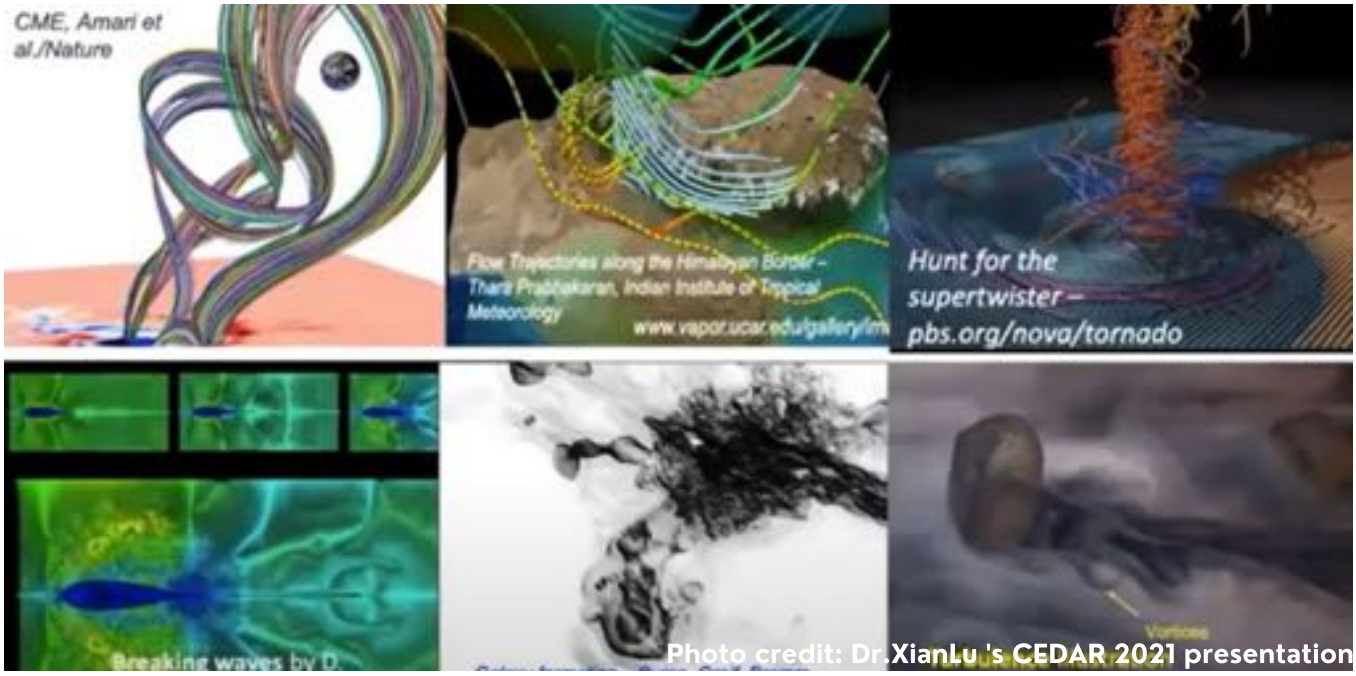

Photo credit: Dr.XianLu 's CEDAR 2021 presentation

INTRODUCTION

Atmospheric Models are mostly numerical models that are used to generate physical and numerical quantities and parameters in order to quantify the changes in atmospheric phenomena over space and time. There are many applications of numerical modeling, from the simulation of Coronal Mass Ejection (CME) to the study of Breaking wave and Galaxy Formation, as well as Turbulence Illustration.

The numerical modeling is basically controlled by ordinary and partial differential equations such as wave equations, heat conduction/heat diffusion equations, Laplace equation, and Maxwell's equations. Because the atmosphere is gas (fluid), it obeys the fundamental dynamics of fluid which are the Navier-Stokes equation and the continuity equation.

Wave equations:

$$\frac{\partial \psi}{\partial t} + c\frac{\partial \psi}{\partial x} = 0 \qquad \text{Solution: } \psi = f(x - ct)$$

Heat conduction/diffusion equations:

$$\frac{\partial f}{\partial t} = k\left(\frac{\partial^2 f}{\partial x^2} + \frac{\partial^2 f}{\partial y^2} + \frac{\partial^2 f}{\partial z^2}\right)$$

Laplace Equation:

$$\left(\frac{\partial^2 \psi}{\partial x^2} + \frac{\partial^2 \psi}{\partial y^2} + \frac{\partial^2 \psi}{\partial z^2}\right) = 0$$

Maxwell's Equation:

E and B	E, B, D, and H
$\nabla \cdot \mathbf{E} = \frac{\rho}{\epsilon}$	$\nabla \cdot \mathbf{D} = \rho$
$\nabla \cdot \mathbf{B} = 0$	$\nabla \cdot \mathbf{B} = 0$
$\nabla \times \mathbf{E} = -\frac{\partial \mathbf{B}}{\partial t}$	$\nabla \times \mathbf{E} = -\frac{\partial \mathbf{B}}{\partial t}$
$\nabla \times \mathbf{B} = \mu \mathbf{J} + \frac{1}{c^2}\frac{\partial \mathbf{E}}{\partial t}$	$\nabla \times \mathbf{H} = \mathbf{J} + \frac{\partial \mathbf{D}}{\partial t}$

Fundamentally, the starting point of any numerical model is the set of partial differential or integral differential equations and boundary conditions. A solution method is usually designed for a particular set of equations. After selecting the partial differential equations, one has to choose a suitable discretization method. The discretization method follows by approximating the differential equations by a system of algebraic equations for the variables at some set of discrete locations in space and time. There are many approaches, but the most important of which are finite difference (FD), finite volume (FV), and finite element (FE) methods. Each type of method yields the same solution if the grid is very fine.

The discrete locations at which the variables are to be calculated are defined by the numerical grid which is essentially a discrete representation of the geometric domain on which the problem is to be

solved. It divides the solution domain into a finite number of subdomains (elements, control volumes, etc.). Generally, numerical modelings can be used to advance to the future space and time, by knowing the initial conditions and boundary conditions. In terms of approximations to derivatives, there are different ways to get the true solution of the slope at a certain location.

Fundamentals of Numerical Modeling

The spacial and temporal atmospheric continuity can be described by Partial Differential Equations (PDEs), which to some extent dominates the atmospheric physics system. However, due to the complexity of PDEs, many times it's impractical to find the analytical solutions, thus, we may try to compute the solutions numerically. The solutions of PDEs are often obtained by using digital computers. For example, if one PDE involves mathematical operations like integration, then the analytic processes of integration must be replaced by a numerical method that can yield an approximation to the true solution.

Finite difference (FD) approximations to derivatives

A finite-difference is a mathematical expression of form: f (x + b) − f (x + a). The approximation of derivatives by finite differences plays a central role in finite difference methods for the numerical solution of differential equations, especially boundary value problems.

The starting point is the conservation equation in differential form. The solution domain is covered by a grid. At each grid point, the differential equation is approximated by replacing the partial derivatives by approximations in terms of the nodal values of the functions. The result is one algebraic equation per grid node, in which the variable value at that and a certain number of neighbor nodes appear as unknowns. In principle, the FD method can be applied to any grid type. However, in all applications of the FD method known to the authors, it has been applied to structured grids. The grid lines serve as local coordinate lines. On structured grids, the FD method is very simple and effective. It is especially easy to obtain higher-order schemes on regular grids.

To obtain an approximate solution numerically, we have to use a discretization method which approximates the differential equations by a system of algebraic equations, which can then be solved on a computer. The approximations are applied to small domains in space and/or time so the numerical solution provides results at discrete locations in space and time.

Different numerical schemes

Some of the numerical schemes employed in atmospheric sciences include the following: Runge-Kutta, Lax-Wendroff, Spatial Filtering, and Corner Transport Upstream

Runge-Kutta numerical scheme is a temporal scheme in which there are 3 or 4 minor steps in order to better approximate the slope of the temporal tendency. Corner Transport Upstream (CTU) method, in addition to adopting the regular different scheme, it also has a factor that can compensate for the truncation error on the RHS.

Finite difference vs Finite volume

All the different schemes compared above fall with the finite difference, which means the values and derivatives are evaluated at discrete grid points. The finite volume method uses the integral form of the conservation equation as the starting point. The solution domain is subdivided into a finite number of small control volumes (CVs) by a grid which, in contrast to the finite difference (FD) method, defines the control volume boundaries, not the computational nodes. The usual approach is to define CVs by a suitable grid and assign the computational node to the CV center. However, one could as well (for structured grids) define the nodal locations first and construct CVs around them, so that CV faces lie midway between nodes. The advantage of the first approach is that the nodal value represents the mean over the CV volume to higher accuracy (second-order) than in the second approach since the node is located at the centroid of the CV. The advantage of the second approach is that CDS approximations of derivatives at CV faces are more accurate when the face is midway between two nodes.

Examples of Atmospheric Models

1. Empirical models are based on statistical and mathematical data

Good for climatology and background atmosphere, such models include NRLMSIS, IRI, Horizontal Wind Model (HWM), Weimer, Heelis, and Ovation.

Naval Research Lab Mass Spectrometer Incoherent Scatter (NRLMSIS) model is basically a whole-atmosphere empirical model of temperature and neutral species densities. The NRLMSIS 2.0 is an empirical atmospheric model that extends from the ground to the exobase and describes the average observed behavior of temperature, 8 species densities, and mass density via a parametric analytic formulation. The model inputs are location, day of the year, time of day, solar activity, and geomagnetic activity. Some outputs of NRLMSIS are shown in Fig.1.

International Reference Ionosphere (IRI) model is an international project sponsored by the Committee on Space Research (COSPAR) and the International Union of Radio Science (URSI).

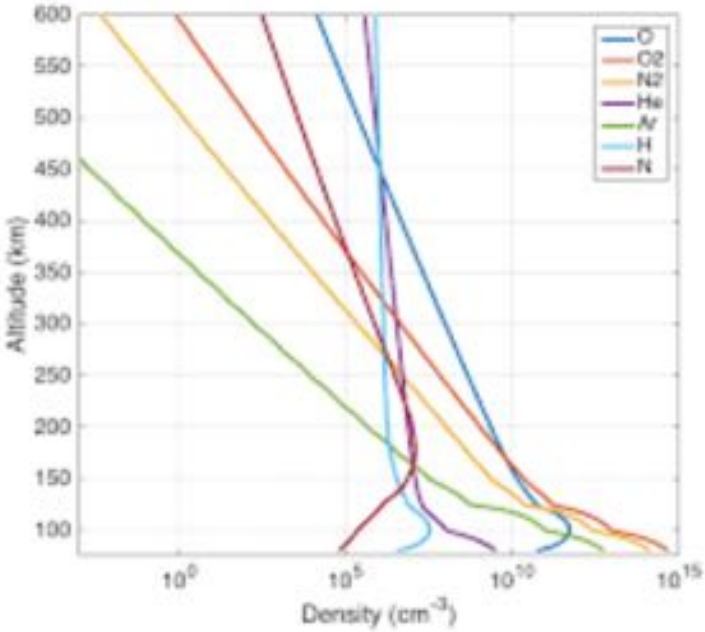

Fig.1: Some output of NRLMSIS model.

The IRI model is an empirical model used to provide the following outputs: electron density (Ne), electron temperature (Te), ion temperature (Ti), ion composition, equatorial VI, vertical TEC, spread-F probability, auroral boundaries, effects of ionospheric storms on F and E region peak densities. The model inputs require solar indices (F10.7), ionospheric index (ionosonde-based IG index 12-month running mean), and magnetic index (ap).

2. Physics (physical) models

Steady-state models in which the mean values or wave amplitude do not change with time, and they involve external forcing or boundary conditions. Examples of the steady-state model include: GSWM, CTMT.

Global Scale Wave Model (GSWM) is used to investigate the effects of mean winds and realistic dissipation on upward propagating nonmigrating diurnal tidal components. An advantage of GSWM is the fact that it has an integer wave number, and also has a predictable periodic oscillation for tides.

Climatological Tidal Model of the Thermosphere (CTMT) involves the generalized form of Hough Modes which accounts for dissipation. This model concept entails fitting the Hough Mode Extensions (HMEs) to TIMED tides in the MLT region, and also use fit coefficients to reconstruct the tides in the thermosphere with the solar flux index (F10.7) being equal to 110SFU.

Stationary Planetary Wave Model which does not change with time, allowing us to basically get ride of t. The stationary planetary wave model usually has a complex solution that is forced by a lower boundary condition.

The numerical scheme is based on the refractive index square (Qm). This parameter is determined by background atmospheric statuses such as wind and temperature.

The modeling results are very sensitive to the refractive index square, in the sense that, the waves stop propagating when the refractive index square has a negative value ($Qm<0$), which implies that the wave is absorbed or reflected.

Time-evolving Models involve initial conditions the dynamic networks that are the typical language for describing time-evolving complex systems, and discrete-time network models provide an emerging statistical technique with stability for various applications.

The general circulation models which include: CESM, KMCM, TIEGCM, CTIPe
Thermosphere Ionosphere Electrodynamics General Circulation Model (TIEGCM) uses the finite difference scheme such as the Leapfrog scheme which leads to zonal and meridional momentum equations. This model applies the Spatial filtering with Shapiro constant c=0.3.

Community Earth System Model (CESM) is a fully coupled, global climate model that provides state-of-the-art computer simulations of the Earth's past, present, and future climate states.

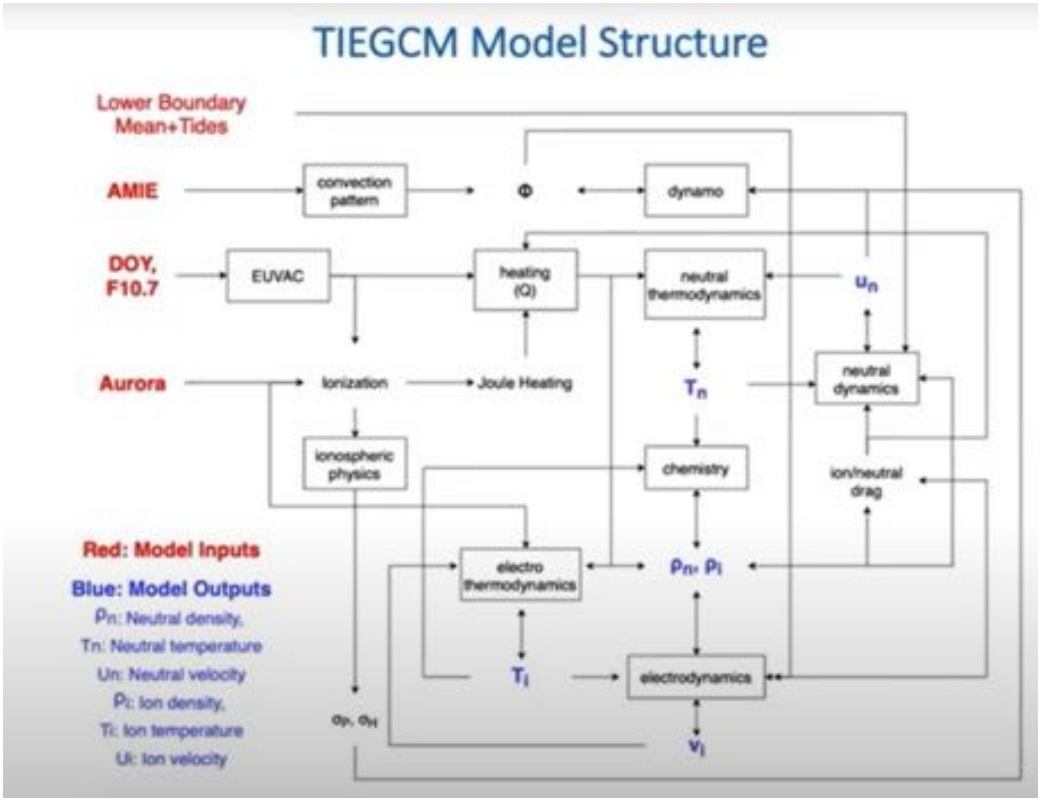

Fig.2. Illustration of the TIEGCM model structure

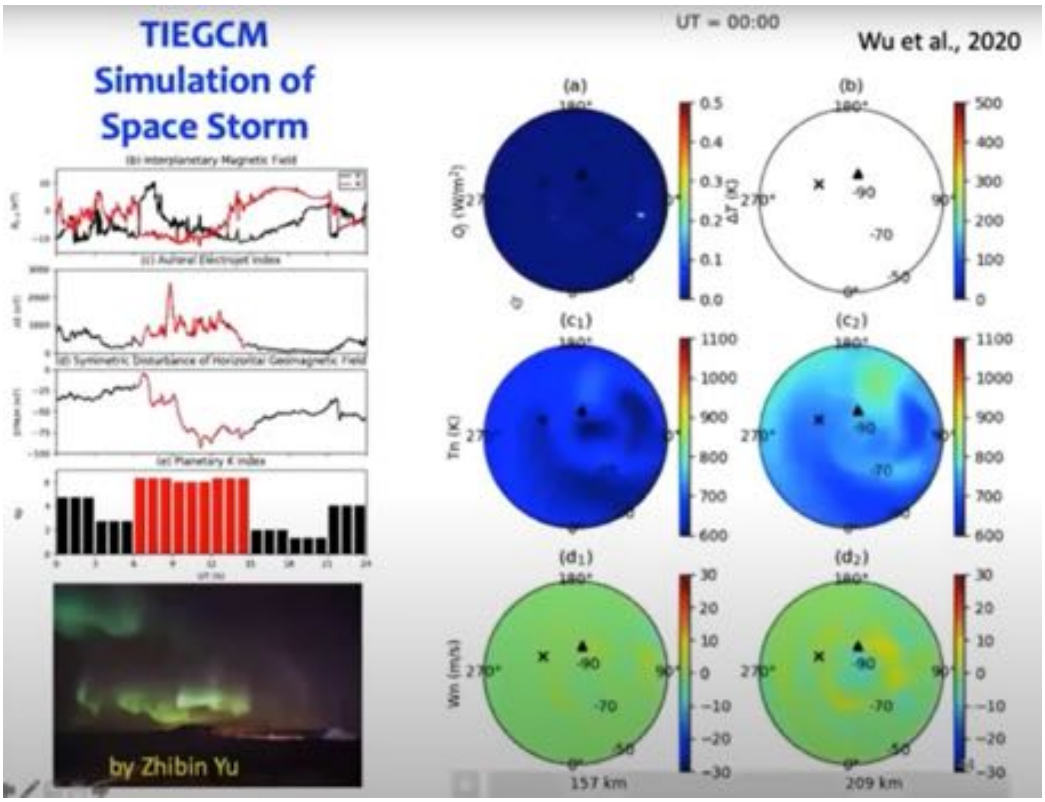

Fig.3. An example of of the TIEGCM model simulation.

Barotropic/baroclinic planetary wave model and Gravity wave models such as Model for Acoustic Gravity wave Interaction and Coupling (MAGIC). The MAGIC is a 2D model that solves non-linear, fully compressible, Euler equations with the inclusion of the effects of molecular and thermal conductivity.

3.Data assimilation models

Underlying Physics models + data assimilation
WACCM-DART, ECMWF, MERRA
In summary, numerical models are useful to explain observations, fill up observational gaps, and study physical mechanisms. They are also employed in the prediction of hazardous weather, space weather, climate change, etc., and can be involved in advanced theories that account for missing physics components.

Speaker bio

Dr. Xian Lu is an assistant professor in the department of physics and astronomy, Clemson University. Her research focuses on atmospheric waves and magnetosphere-ionosphere-thermosphere coupling using numerical modeling and observations. She is the recipient of NSF CAREER award and "Rising Star in Discovery" award at Clemson.

ION-NEUTRAL COUPLING

DR. TOSHI NISHIMURA, BOSTON UNIVERSITY
SUMMARY WRITTEN BY JOAQUIN DIAZ PENA

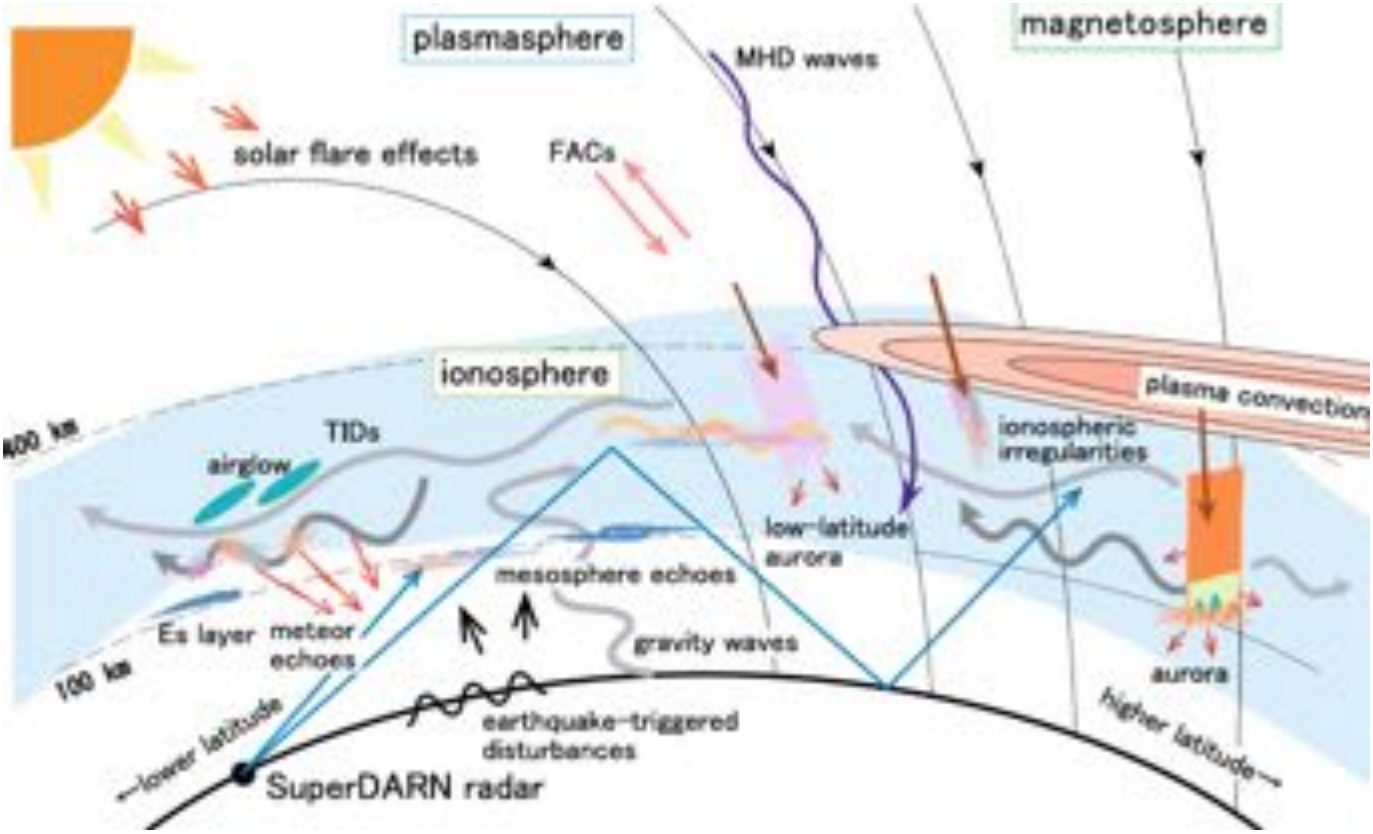

INTRODUCTION

Ion-Neutral coupling is a common theme for several back-to-basics sections (Joule Heating, Sudden Stratospheric Warming, Acoustic Waves). More details and specific topics can be found there. Here, we will go over an overview of it, basic equations, and some examples.

Importance

The ISS is a well-known platform in orbit, it is constantly falling due to the thermosphere density. Sudden descents can happen during storms, where it can fall by approximately 150m. This is due to the energy exchange between ions and neutrals, which cause an enhanced thermosphere density by heating and

transport. Physical understanding of the ion-neutral coupling is vital for space weather, and ion-neutral coupling is considered an important topic at a national level.

Equations

Momentum equation for the neutrals: describes the changes in wind speed due to ion drag force, pressure gradients, Coriolis, and other forces. When ions and neutral collide the velocity difference between the plasma and neutrals drives the neutral wind, with the collision frequency as a factor between them. Energy equation for the neutrals: describes the evolution of pressure, as it changes with the chemistry, heat exchange between ions and neutrals, heat exchange between electron and neutrals, as well as the velocity difference between neutrals and ions. This last one is particularly called Joule Heating and its energy is coming from the Poynting flux supplied from the magnetosphere.
Current continuity describes the relation between three key parameters: J|| associated to the field align currents, Σ associated with the conductance in the ionosphere, and E associated with the convection. The conductance comes from the solar EUV and the auroral oval precipitation, and have the form shown below:

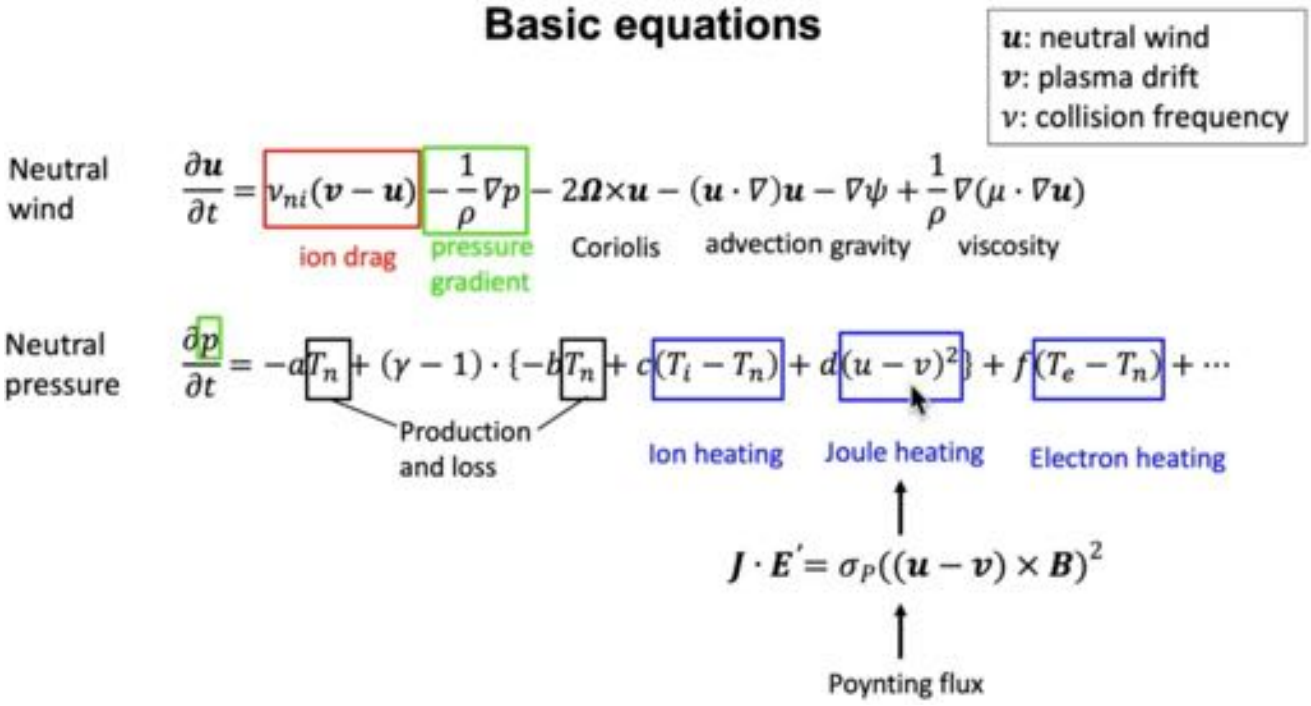

Pedersen conductivity $\sigma_P = \left(\frac{\nu_{en}}{\nu_{en}^2 + \omega_{ge}^2} + \frac{m_e}{m_i} \frac{\nu_{in}}{\nu_{in}^2 + \omega_{gi}^2} \right) \frac{n_e e^2}{m_e}$

Hall conductivity $\sigma_H = -\left(\frac{\omega_{ge}}{\nu_{en}^2 + \omega_{ge}^2} + \frac{m_e}{m_i} \frac{\omega_{gi}}{\nu_{in}^2 + \omega_{gi}^2} \right) \frac{n_e e^2}{m_e}$

Plasma-neutral coupling
ν_{in}: Ion-neutral collision frequency
ν_{en}: Electron-neutral collision frequency

Wind accelerations examples

Neutral wind by ion drag $\frac{\partial \boldsymbol{u}}{\partial t} \sim \nu_{ni}(\boldsymbol{v} - \boldsymbol{u}) - \frac{1}{\rho}\nabla p - 2\boldsymbol{\Omega}\times\boldsymbol{u}$

ion drag | pressure gradient | Coriolis

Plasma drift

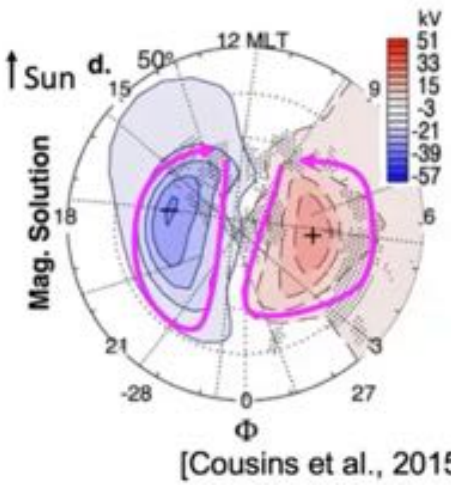

[Cousins et al., 2015]

Neutral wind

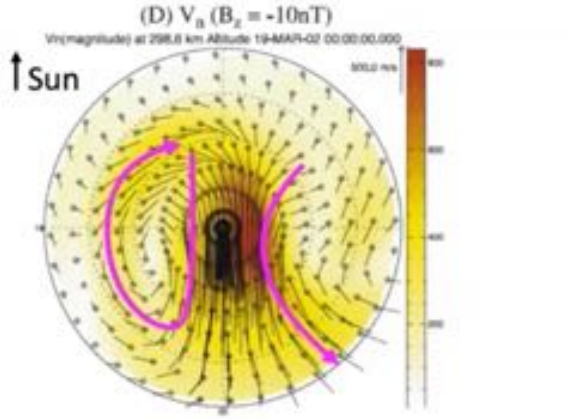

[Deng et al., 2006; Forster et al., 2008]

On the left we have the two-cell convection pattern of the plasma, and on the right the neutral wind on the same format. Interestingly the neutrals also have a two-cell convection pattern, this is because the ion drag force mentioned earlier. Except in the dawn side, where other forces contribute to a greater capacity, with Coriolis force trying to turn the wind westward.

The ion neutral collision frequency is also important because the inverse of it tells you the acceleration time scale. This is usually long, 10s of minutes to hours as opposed to the plasma acceleration time scale where it changes in minutes due to magnetospheric inputs. When the magnetospheric inputs weaken, plasma drift quickly decays but neutral wind is still strong. In this case the neutral wind accelerates the plasma (Flywheel effect).

Another important point is that neutral wind acceleration scale is highly variable, because of the ever-changing magnetospheric energy input. A sudden plasma density enhancement shortens the acceleration time scale and rapidly accelerates the wind. It is important to understand the dynamic variability of the magnetospheric energy input to understand the neutral wind dynamics.

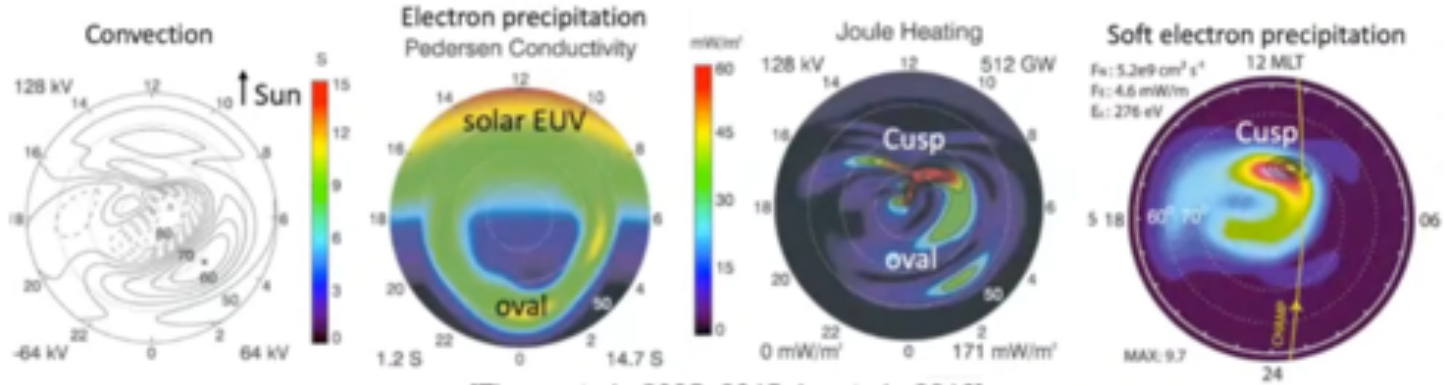

[Zhang et al., 2005, 2015; Lu et al., 2016]

Heating

On the pressure equation the Joule Heating term depends on the Pedersen conductivity which is enhanced in the auroral oval and regions with solar EUV. Not only the high energy precipitation in the auroral oval contributes to Joule Heating, but low energy precipitation in the cusp region as well. As such, Joule Heating peaks in the cusp region and is moderately enhanced in the auroral region. Particle precipitation itself also heats up the plasma as seen in the other two terms of the pressure equation. These three heating terms contribute to the neutral heating.

Influence on low-mid latitudes

Winds created by heating in the auroral oval are not local to the auroral oval, and they can propagate away from the oval itself equatorward with a westwards trend due to Coriolis force. The wind then modifies the thermospheric composition and chemistry of the atmosphere for major species. The wind also drags plasma from the high latitudes to the lower latitudes creating additional electric fields at those latitudes. The signal can also propagate waves of neutral density as Traveling Atmospheric Disturbances (TAD). The plasma density is also perturbed by the ion drag as Traveling Ionospheric Disturbances (TID). Even though the lower latitudes are far away from the auroral oval, the ion-neutral coupling in the auroral oval affects the lower latitudes ion-neutral processes. It is important to understand the global picture. Tidal waves in the equatorial plasma density are affected by both TID and TAD, where otherwise other explanation for these kinds of effects could not be solved by just looking at the magnetospheric input.

Future

The future of ion neutral coupling has still many unknown issues. NASA plans to launch GDC in 2027 and ion-neutral coupling is a key part of this mission, with several science objectives related to it:

- Determine how the plasma convection and precipitation drive neutral winds
- Determine how neutral winds, precipitation, and heating drive neutral density structures
- Determine the relative importance of penetration electric fields and disturbance winds
- Intensify the processes that create and dissipate propagating structures within the ionosphere and thermosphere (TAD/TID)

Speaker bio

Dr. Toshi Nishimura got his PhD at Tohoku University, Japan in 2009. He worked at UCLA as a researcher until 2016, and he is now a research associate professor at Boston University. He received the AGU Outstanding Student Paper Award in 2007, the URSI Young Scientist Award in 2015, and AGU Macelwane Medal in 2016. He is currently the lead of the CEDAR Grand Challenge session on Multi-scale ionosphere-thermosphere system, and his research interests are magnetosphere-ionosphere coupling by auroral imaging.

IRREGULARITIES AND INSTABILITIES

DR. TITUS YUAN , USU
SUMMARY WRITTEN BY ZISHUN QIAO

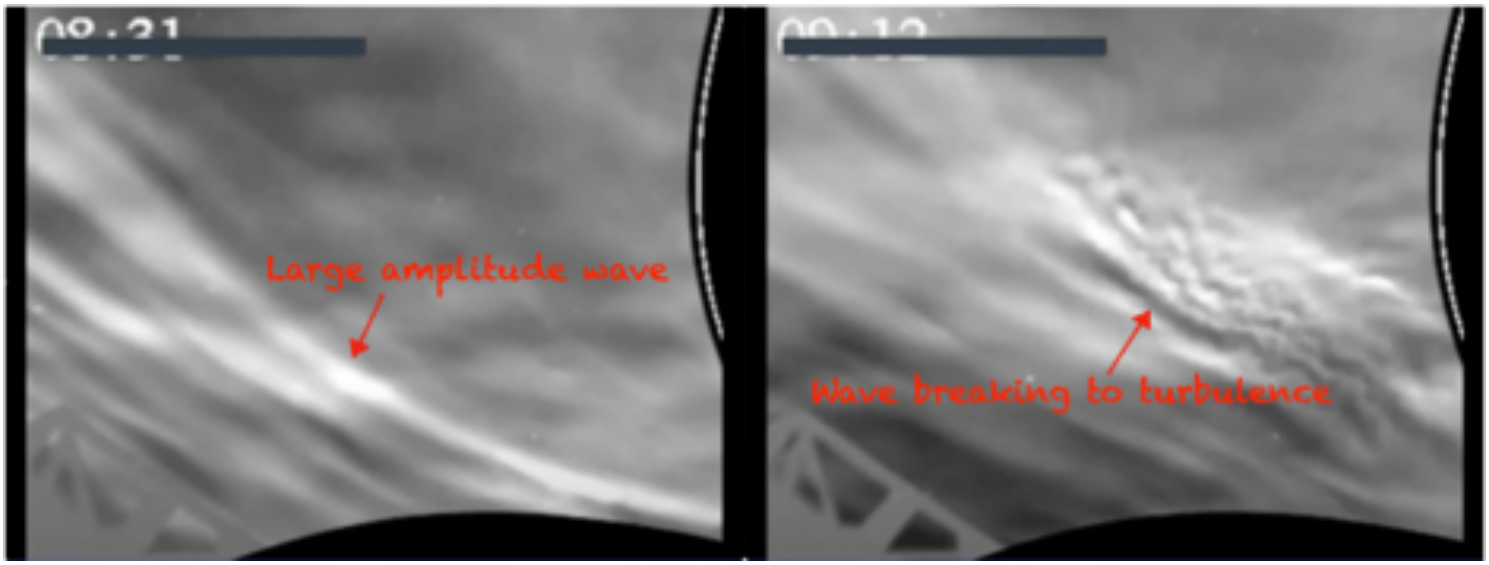

Credit: Dr. Yuan Slide, CEDAR workshop 2021

Dr. Yuan introduced the physical concepts of atmospheric instability by firstly showing a real-world movie of a chaotic wave breaking, captured by the advanced atmospheric temperature mapper at Utah State University.

How do we quantitatively understand atmospheric instabilities?

The Brunt-Väisälä frequency square, defined as

$$N^2 = -\frac{g}{\rho}\frac{\partial \rho(z)}{\partial z}$$

is one of the key parameters used to study atmospheric stabilities. If N^2 is positive, the atmosphere is statistically stable, however if N^2<0, we will have statical instability.

Dr. Yuan introduces this famous quantity starting from talking about hydrostatic equilibrium -- the weight of the packet of air is balanced by the net pressure force. If we push the packet of air away from its equilibrium position by a small distance in z direction, the buoyancy force given by the newton second law will lead us to the solution including $i\sqrt{N^2}$ as the complex exponential index. Thus, we have the sign discussion of the Brunt-Väisälä frequency square.

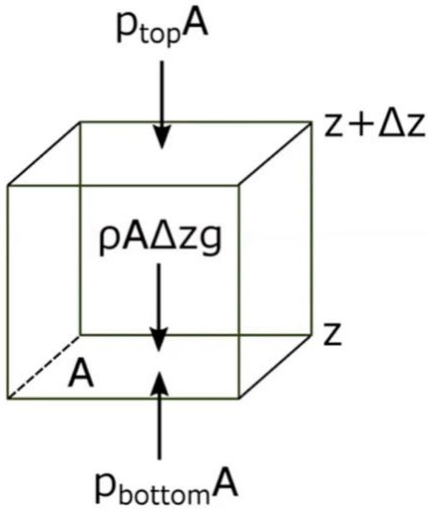

Because the gravitational force acts opposite to the upward-directed pressure gradient force, the packet of air remains in a state of equilibrium called "hydrostatic balance."
Credit: Dr. Yuan Slide, CEDAR workshop 2021

Richardson number is another key parameter to study turbulence. Defined as $R_i = N^2/SH^2$, where SH is the magnitude of the wind shear, Richardson number describes a competition between the positive static stability (N^2>0) who prevents the vertical displacement and the vertical wind shear who causes Kelvin-Helmholtz instability (KHI) and thus leads to the vertical mixing. When Ri>1/4, static stability winds and perturbations are stable (dynamic stability). When Ri<1/4, either through reduced static stability or increased wind shear, the perturbations may change to turbulence (dynamic instability).

In addition, Dr. Yuan reminds us the concept of **Reynolds number** (Re) that defined as the ratio of inertia force and viscous force of the flow in fluid dynamics, which is a key tool used to determine the stability of a flow. In other words, Reynolds number helps us figure when will the flow change from laminar flow to turbulent flow. When Re<2300, we have orderly laminar flow going in the same direction with less interaction with the background; when Re>4000, chaotic turbulent flow exists, interacts with the background and deposits the original energy and momentum into the background. In between of both we have transient flow with characteristics of a little of both.

Importance of atmospheric instabilities

- Atmospheric instabilities play important roles in upper atmospheric dynamics and ion-neutral coupling processes. They also contribute to ionosphere irregularities, especially the variations of midlatitude sporadic E layers in the ionosphere E region, locally and globally.

- Atmospheric instabilities induce wave breaking and thus cause the deposition of energy and momentum carried by the waves in our dynamically coupled atmosphere.

- The turbulence processes are everywhere with all sorts of spatial and temporal scales, however our state-of-the-art simulations still rely on gravity wave parameterization to resolve turbulence processes. Progress has been made to directly measure the turbulence, but only limited to a few ground-based observations.

Speaker bio

Dr. Titus Yuan received his PhD from Colorado State University in 2004. Currently, he is an Assistant Professor in the Physics Department at Utah State University. He has been the leading PI of the Utah State University sodium lidar project since 2010, working on the development, deployment and operating of sodium lidar system. His work enables the robust, reliable daytime sodium lidar observation capability.

AN OVERVIEW OF SUDDEN STRATOSPHERIC WARMINGS

DR. NICK PEDATELLA , HAO/NCAR
SUMMARY WRITTEN BY ZISHUN QIAO

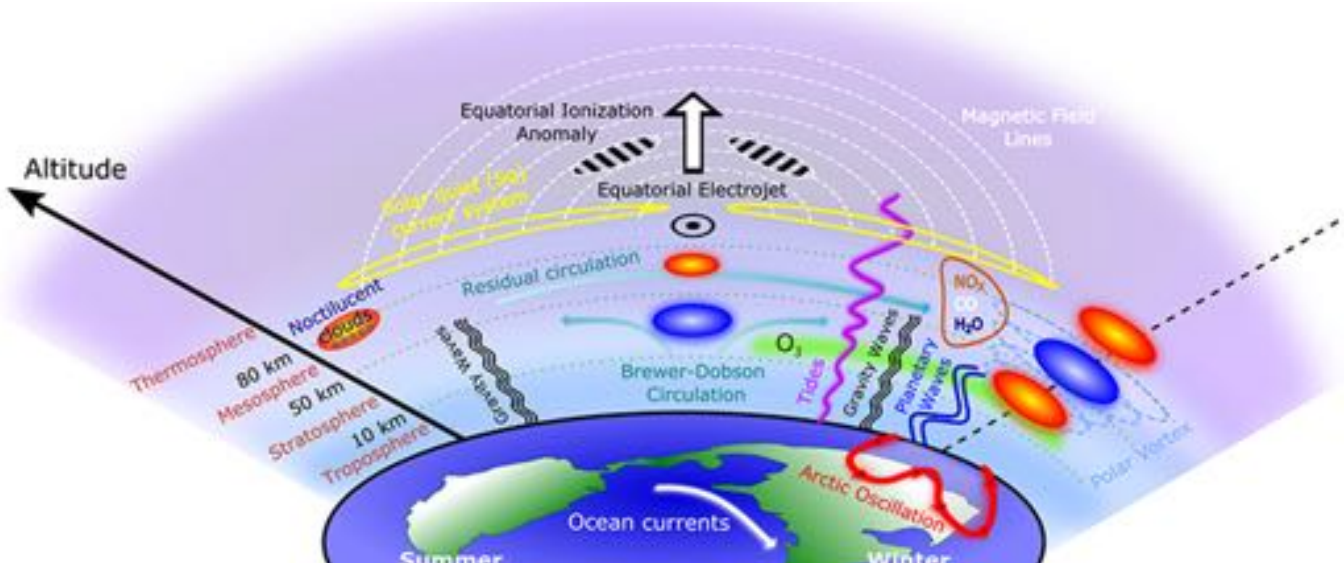

Fig. Schematic of the coupling processes and atmospheric variability that occur during sudden stratospheric warming events. Red and blue circles denote regions of warming and cooling, respectively. Credit: Pedatella et al., 2018

INTRODUCTION

Sudden Stratosphere Warmings (SSWs) are dynamical disturbances in the high latitude wintertime stratosphere that influence the whole atmosphere. During SSWs, stratospheric temperatures can fluctuate by more than 50°C over a matter of days. SSWs have several characteristic features, including: (1) warming of the high latitude stratosphere, (2) cooling of the mesosphere, (3) warming of the lower thermosphere and (4) deceleration and, during major SSWs, reversal of stratospheric winds. Dr. Pedatella introduced such impacts of SSWs based on some results of composite model simulations.

What's the mechanism underlying the formation of SSWs? SSWs are generated by the interaction of planetary waves and the zonal mean flow, and occur ~6 times per decade on average in the Northern Hemisphere. However Southern Hemisphere SSWs are rare due to less land-sea contrast and thus weaker planetary wave activity in the Southern Hemisphere.

Impacts of SSWs on the middle and upper atmosphere

First of all, amplitudes of the semidiurnal solar and lunar atmospheric tides increase significantly during SSWs. Atmospheric tides are global scale periodic oscillations that are driven by solar heating, latent heat release due to deep convection, and lunar gravity. Mechanisms of tidal enhancements during SSWs are: (1) change in propagation due to changes in zonal winds, (2) change in generation of solar semidiurnal tide due to changes in stratospheric ozone, (3) non-linear interaction between tides and planetary waves and (4) shift in resonance mode of the atmosphere towards the period of the lunar tide.

These changes in solar and lunar tides during SSWs can modulate the E-region dynamo, which leads to large changes in the low latitude ionosphere, especially in terms of the vertical plasma drift. And the changes in equatorial plasma drifts will impact low latitude ionosphere electron density. During SSWs, total electron content (TEC) can change by 50-100%, which is a similar magnitude to a moderate geomagnetic storm. Dr. Pedatella showed us a case of Jicamarca ISR observation during 2009 SSW in this talk.

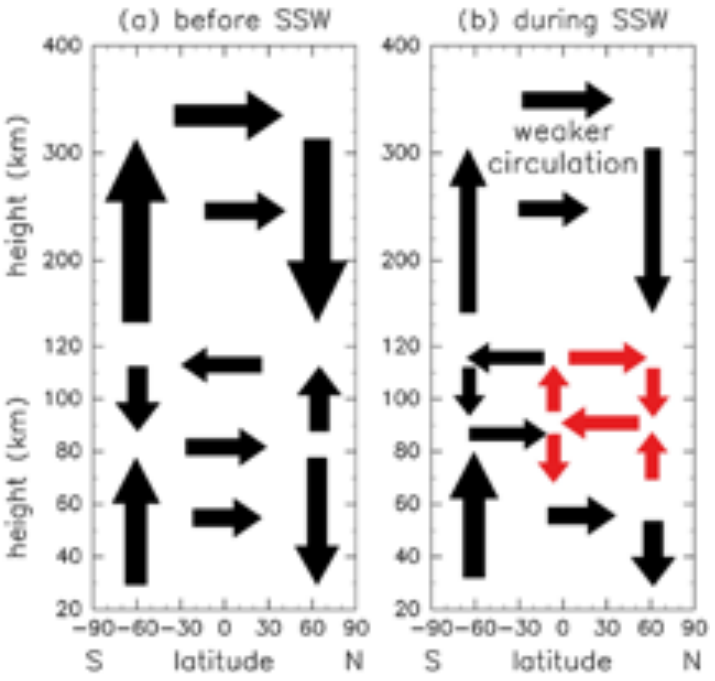

Figures illustrating meridional circulation (a) during the pre-SSW period and (b) during the SSW period. Credit: Miyoshi et al., 2015

In addition, major SSWs can even alter the mean flow circulation pattern in the middle-upper atmosphere, due to the wave dissipation such as gravity waves, planetary waves, and tides during SSWs. This leads to a variety of effects: (1) Circulation changes can alter the chemistry of the middle atmosphere, such as increasing the downward transport of nitric oxide. For example, the downward transport of NOx (NO+NO2) is enhanced in winters during strong SSWs. Since NOx can destroy ozone in the stratosphere, this leads to potential effects at lower altitudes. (2) Circulation changes lead to a decrease in atomic oxygen (O) in the lower thermosphere, and then molecular diffusion will propagate this

decrease into the upper atmosphere, which can be observed as the decreased O/N2 ratio. (3) Wave dissipation can also lead to a reduction in thermosphere density (atmospheric drag) and temperature.

Forecast of SSWs

The good forecast skill of SSWs offers the potential for extended space weather forecasting, at least during solar and geomagnetic quiet time periods. The occurrence of SSWs can be forecast ~10 days in advance, with individual events exhibiting better/worse forecast skill. More specifically, extended forecasts of IT variability during SSWs may be made possible given the ability to forecast the tidal variations. Dr. Pedatella gave us an example of analysis of 14 SSWs in initialized Whole Atmosphere Community Climate Model (WACCM) hindcasts, which demonstrates ability to forecast semidiurnal tide variations during SSWs.

Outstanding Questions

- How does the ITM response to SSWs vary with longitude, and what are mechanisms generating longitudinal variability?
- Is there a connection between SSWs and ionospheric irregularities?
- How do SSWs influence the generation and propagation of gravity waves and the formations of TIDs?
- How does the ITM response to periods when the stratospheric vortex is strong (i.e., the opposite of SSWs)?

Speaker bio

Dr. Nick Pedatella is a scientist at the National Center for Atmospheric Research, High Altitude Observatory. He received his Ph.D. from CU Boulder in 2011. His primary research interest is understanding the influence of lower atmospheric waves on the spatial and temporal variability of the upper atmosphere. His research is conducted using a variety of satellite observations and numerical models. He is additionally interested in the development and application of data assimilation techniques as a means to better constrain numerical models. His current research also focuses on developing improved techniques for remote sensing of the ionosphere using Global Navigation Satellite System observations.

PLANETARY ATMOSPHERES

DR. CHENG LI, THE UNIVERSITY OF MICHIGAN
SUMMARY WRITTEN BY MEGHAN LEMAY

The last talk of the day was given by Dr. Cheng Li of the University of Michigan on Jupiter's Great Red Spot (GRS). The GRS is both an old and new topic. It is old because it was first seen with telescopes in the 1800s, and it is new because only recently has enough information been gathered to answer many of the questions scientists have about its existence. What is the equivalent of the GRS in terms of Earth's atmosphere? It is an enormous anti-cyclone or hurricane with a calm center. For the past twenty years, there has been continuous observations of the phenomenon, and scientists have noticed its evolution and shrinking. It is unknown if the GRS will fully disappear over time, but at the rate it is shrinking it will be gone in forty to fifty years. There is no definitive answer on how it formed, but modeling using a single-layer atmosphere has shown that small perturbations from zonal jets combine to form a large vortex. The GRS might be explained using the Taylor-Proudman Theorem in fluid dynamics where fluid goes around a region where an obstacle is. With regards to the internal structure, scientists have been

speculating that there is a cold core top, a midplane with cloud structures, and a hot bottom layer, but without measurements, no one can say for certain.

The Juno mission is the first mission that goes inside the radiation belt of Jupiter. The Juno spacecraft is equipped with six microwave antennas that measure the radiation of Jupiter at significant wavelengths. These wavelengths cannot be seen from observations of Jupiter so measurements must be taken within the radiation belt. Fortunately, the Juno spacecraft flies over the middle of the GRS. Measurements from Juno more or less confirm the hypothesis that the top of the GRS is cool, and the bottom is hotter with the added complication of a bifurcation with the north part being warm and the south part being cold.

The atmosphere of Jupiter emits thermal radiation. The thermal radiation passes through a layer of absorbing molecules of ammonia gas. As a result, the absorbed thermal radiation is what reaches the antenna on the spacecraft. This quantity is called the brightness temperature. If a higher brightness temperature is observed, there are two explanations. The first is that the actual temperature of the atmosphere is high. The other explanation is that the amount of absorbing molecules is low. The density of the atmosphere is mostly determined by the temperature and only slightly influenced by the composition. Remote sensing techniques are employed to de-convolve the contribution from the temperature and the contribution from the distribution of absorbing species. This can be done using MCMC inversion using Rectified Gaussian Process which shows which combination of temperatures and densities can explain the observations. This process is used to determine the background ammonia concentration based on restrictions placed on the temperature distribution. The results show that the GRS is warm at the north and cold at the south with a very enriched ammonia concentration at the north. The model has shown to reproduce the observations extremely well. Additionally, comparing the background ammonia to the ammonia within the GRS shows that the ammonia within the GRS is vertically layered which may mean that the GRS is a rigorously convecting system which can explain why the north is warmer than the south via adiabatic expansion and compression. This is a north-south asymmetry.

Speaker bio

Dr. Cheng Li is currently an assistant professor of University of Michigan, Ann Arbor. He received his Ph.D. degree in Planetary Science at California Institute of Technology in 2017, spent 2 years at Jet Propulsion Laboratory working on the Juno mission as a NASA Postdoctoral Program fellow. Then he spent 3 years at University of California, Berkeley as a 51 peg b fellow. His main research interest is fluid dynamics, especially atmospheric dynamics.

DEI CALL TO ACTION

DR. MCARTHUR JONES, NRL
SUMMARY BY MEGHAN LEMAY

The Diversity, Equity, and Inclusion (DEI) Task Force has been meeting throughout the year to discuss and improve DEI related issues within CEDAR. The task force was started last year as a spin-off from the DEI in CEDAR session at the 2020 CEDAR Workshop when conveners of the session got feedback about some of the DEI issues within CEDAR. The task force has three goals: assess and formalize DEI efforts within CEDAR, establish and normalize a DEI presence within CEDAR, and foster improvement through implementation of DEI action items. The task force's top action items for this past year are including demographic questions on CEDAR's registration forms, creating a safe space for members of CEDAR to discuss DEI related issues, creating a group to proofread letters of recommendation for bias, creating connections with institutions that serve diverse students, connecting with high school students, and creating the CEDAR Outstanding Mentor Award. If you would like to get involved with DEI in CEDAR, there are several ways you can. The first step is to sign the DEI Statement and Call to Action. To participate in DEI events, please join the DEI Task Force's happy hours or contact anyone on the task force to learn more about participation. If you are experiencing any DEI issues, please feel free to reach out to anyone on the task force.

QUESTIONS AND ANSWERS

COLLECTED BY MEGHAN LEMAY & ZISHUN QIAO

- Incoherent Scatter Radar
- Meteor Radar
- Optical Instruments
- Satellites: Past Present and Future
- Hierarchy of Atmospheric Models
- Ion-Neutral Coupling
- Joule Heating
- An Overview of Sudden Stratospheric Warmings
- Acoustic Waves

Incoherent Scatter Radar (ISR) - by Dr. Ashton Reimer (SRI)

Q: What is the total observation area for ISR radar like PFISR and millstone hill?

A: Great question. In general, the field-of-view (FOV) for each radar is different for reasons that depend mostly on differences in hardware. Millstone Hill uses dish-type antennas. For the zenith antenna, which is fixed, can only create altitude profiles. In contrast, the Millstone Hill steerable antenna can point to low elevation angles, which allows it to make measurements at horizontal ranges of ~500 km. This comes with a trade-off, which is that at low elevation angles the FOV doesn't extend as high in altitude.

For the AMISRs, which use phased array antennas, the FOV is limited by how far the beam can be steered without introducing grating lobes. So, we say that how far you can steer the beam depends on the "grating lobe limit", which depends on the antenna spacing and the frequency that the array is operating at. For the AMISRs, at the an operation frequency of ~449 MHz, the antenna spacing is such that the grating lobe limit is approximately +/- 25 degrees off of normal to the array. In addition to the grating lobe consideration, the array may be tilted. PFISR is tilted ~16 degrees to the North such that it can look downrange to the North to support sounding rocket missions from the Poker Flat Research Range. This tilt angle combined with the grating lobe limit enables PFISR to look a couple hundred kilometers downrange.

One important thing to remember is that the FOV of a radar in terms of spatial extent (number of kilometers spanned) is smaller at lower altitudes, such as in the E region, than it is at higher altitudes, such as the F region. This means that it is more challenging make measurements across large areas at lower altitudes than it is at higher altitudes.

A FOV plot for PFISR, in units of degrees azimuth and elevation, can be found here: https://amisr.com/amisr/media/pfisr/pokerazel.jpg. At the top of that plot is geodetic North, with the red dots indicating beam positions and the black outline denotes the grating lobe limit.

Finally, here is a simple figure showing FOVs for different ISRs. The FOVs in this plot are mapped to 300 km. For Millstone, I've assumed the steerable dish was pointed at 30 degrees elevation. Note, that the latitude lines are separated by 10 degrees.

Comparing the PFISR FOV with the RISR FOVs, you can see that the RISRs can look further downrange. This is because their arrays are tilted more steeply than PFISR.

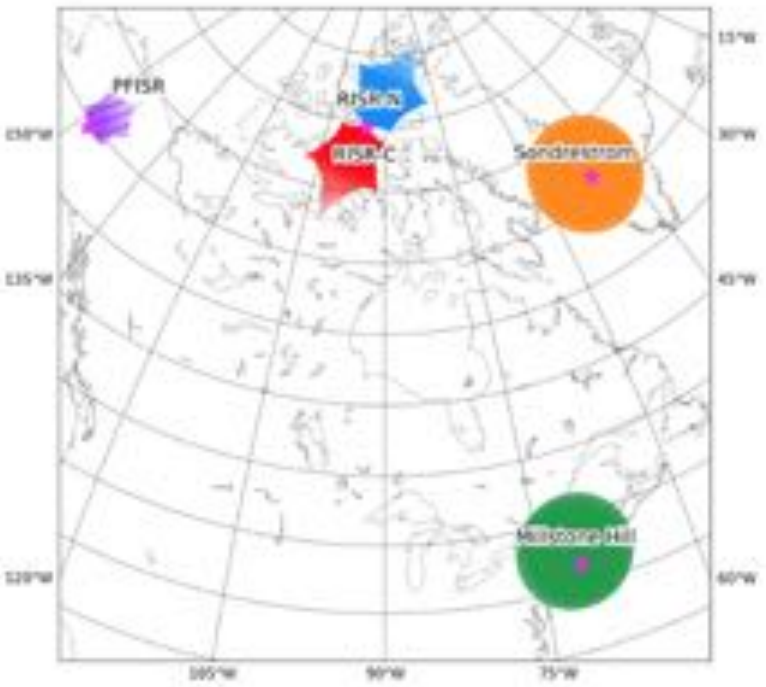

Q: You mention that ISR technique is constantly improved, what are the most recent attempts on including the effects of nonlinear Landau damping?

A: Since ISR requires a broad range of disciplines (electrical engineering, plasma physics, and statistics, just to name a few) there are several ways in which the technique is improving. On the engineering side, current phased array technology allows systems like AMISR to provide 3D volumetric imaging of scalar parameters such as plasma density and temperature.

However, utilizing more advanced phased array technology will enable 3D volumetric imaging of vector parameters, such as the full 3D velocity field. This is what the EISCAT 3D radar system will be capable of (see: https://eiscat.se/eiscat3d-information/).

On the statistics front, there are several improvements that can be and are being implemented to improve the data processing. You may recall from the talk that I mentioned that we usually assume an ion composition when processing the ISR data, but we can do better by using empirical models and statistical methods such as using Bayesian filtering (e.g. https://www.essoar.org/doi/10.1002/essoar.10504337.2).

On the physics front, there are many things that we can do better and these things are often extremely challenging. For example, at high-latitudes during times where there are large electric field strengths, the plasma can be driven into a regime where it is no longer Maxwellian and the velocity distribution can become bi-Maxwellian or even toroidal. When this happens, we need to use completely different models of the ISR spectrum to properly fit the data (e.g. https://agupubs.onlinelibrary.wiley.com/doi/10.1002/2017JA023916).

Answering your question about non-linear Landau damping may require a stronger understanding of the plasma physics literature than I have, but I do know that this is an active area of ionospheric research. For example, there are several studies about a phenomenon called Naturally Enhanced Ion-Acoustic Lines (NEIALs), which manifests as a short (10s of seconds at most) enhancement to the ISR power spectrum due to non-thermal structuring of the plasma. This is suspected to be produced by non-linear plasma processes, such as instabilities (e.g. https://agupubs.onlinelibrary.wiley.com/doi/full/10.1029/2004GL022182). There is also work being done to search for Langmuir cavitons and a suspected relationship to "Medium Frequency Bursts" seen in other RF receivers (e.g. https://agupubs.onlinelibrary.wiley.com/doi/full/10.1029/2011GL050288). Let me close with some final thoughts: All current ISR facilities operate in a narrow range of transmit and receive frequencies, which means they are only capable of probing the plasma with a tiny range of k-vectors. This is like trying to observe a rainbow by looking at only red light.

We know from ISR theory that the shape of the ISR spectrum is different at different k-vectors, similar to how a multi-colored object looks different in different wavelengths of visible light. The ISR community is currently thinking about next-generation ISRs and that has included thinking and discussions about building a facility that can probe the plasma with large k-vector diversity. Such a facility would enable us to do things like unambiguously measure the ion-neutral collision frequency and make independent observations of electron temperature using plasma lines. It would likely also help us better study non-linear plasma processes.

Meteor Radars - by Dr. Ryan Volz (MIT)

Q: Are there certain locations where meteor radars have more detections than others, or “work better” than other locations due to noise factors. E.g. the equator, the poles, etc.

A: This is a great question where the simple answer is “no, all locations pose their unique challenges but none are significantly better than others” and the long answer is much more nuanced.

It's not that there are necessarily more sporadic meteoroids at the equator compared to the poles or vice-versa, but there are differences in what meteors are "easy" to see that couples your location with the season and time of day.

Because of the specular scattering condition, the velocity direction distribution of the meteoroids entering the atmosphere within the meteor radar field of view will have a significant effect on the number of detections. The more atmosphere a meteor has to go through to get to a point where the can see it, the less likely it is to have survived to that point. So you're much less likely to see meteors directly overhead compared to off-zenith. But if you're somewhere where a lot of meteoroids are traveling in that direction, you'll miss a lot. So the main effects are geometric and how that geometry changes with the season or time of day based on where you are on the Earth. This affects what you can see with a particular system design and will result in different diurnal and seasonal patterns in the number of detections. That implies that on some level we would be best served to optimize the viewing geometry of a meteor radar, and especially a meteor radar network, to its location.

Overall, though, the difference in average detection rate for meteors at the equator and those at the poles is not large enough to be a deciding factor in putting a meteor radar at either of those locations.

Q: Do you think there's any research applicability of passive meteor radar using existing HF/VHF sources? I'm sure accuracy is reduced, but I'd expect it would be cheaper and easier to distribute geographically

A: Yes, absolutely! The technique would not be that different from the CW pseudorandom-coded transmitters that I mentioned. The catch is that you need an interferometric array on the receiver side, which is still some work to set up. But any transmitters that are at least sending out a couple hundred Watts of power over ~100 kHz bandwidth would be of good use, and I can definitely see passive links like that becoming important parts of any large network deployment. VHF television transmitters in particular would be a good, somewhat common target for use as a passive meteor radar.

Q: What's the state of the art in meteor radar temperatures derivation? how would the daily and seasonal meteor counts distribution affect it?

A: Temperature estimates are still a somewhat open problem, with not too much recent work that I'm aware of beyond Hocking (1999), 10.1029/1999GL003618 and Hocking et al. (2004), 10.1016/j.jastp.2004.01.01. It's something that I think we should look into more with the wealth of data coming from the new and future meteor radar networks. As with any estimate, the quality will drop when the meteor counts drop, so you'll have slightly worse estimates at sunset than at dawn. But most of the difficulty in estimating reliable temperatures comes from the modeling and assumptions that need to go into it. Any new work on that front would help a lot.

Q: Do smaller meteors affect the measurements you take based off larger ones?

A: Generally, there is no interference, as meteor detections are sparse enough in time and location to not overlap. But there could be situations with meteoroids on very similar trajectories within a very short time window (coming from a common parent, maybe after a breakup). In those cases, one would have to disentangle the echoes using some form of deconvolution of the radar waveform. How well you can do that depends a lot on the waveform and its inherent ambiguity, but there are still techniques like compressed sensing that let you separate the echoes.

Q: Is there any way to detect a meteor that's tail is too small to typically detect with radar? Is there a way to filter the data to find them?

A: Of course there are adjustments you can make to improve detection, such as transmitting more power, using waveform coding to get signal processing gain, or going lower in frequency. Assuming those have been implemented where possible, one can try more sophisticated detection schemes. I'm not aware of too much work to really dig into the data like that, but it would probably involve

modeling the meteor echo and matching it over a longer time period than one would normally do. Essentially, the meteor echo models would form a dictionary of filters!

Finally, there are lots of meteors that you're just not going to detect with a given meteor radar because they come nowhere close to meeting the specular scattering condition. They are forever invisible! You can see these as head echoes with ISR-class radars though, but the field of view is smaller!

Q: Can meteor radar matrix follow one big meteor trail and study the small structure, like turbulence

A: We're not far enough along in deploying such systems to really know what this would look like, but yes, absolutely! You can imagine the specular scattering condition being met for different segments of the trail by different meteor radar links, so you'd be able to see what it looks like at different points in the meteor trail's life. Then you can infer winds at those different points along the trail. You can do even better with a high-power large-aperture radar observing non-specular meteor trail echoes. Those have been used to get the wind as a function of altitude along the trail in very high detail, almost like sending up a sounding rocket to measure the winds!

Optical Instruments - by Dr. Asti Bhatt (SRI)

Q: Is there a central database for all sky data?

A: Sadly, no. There isn't a central database for all-sky data at the moment. Currently, each different all-sky imager or imager network provides data on their own. Images are typically stored as large arrays and hence take up more storage space, so it is challenging to serve them through common community repositories like the CEDAR Madrigal database. While a central database of all-sky data is a good goal to have, an alternative would be to have APIs to access these data using common programming languages.

Q: How difficult is it to remove noise from multi wavelength spectrum?

A: Thanks for the question. It depends on what type of noise you are trying to remove. There is instrument specific noise - like readout noise from the CCD - methods for removing such noise is often outlined by e.g. the CCD manufacturer.

There are other noise sources like e.g. streetlights. If you are trying to observe something geophysical, these noise sources mess up your observations, and can be difficult to remove if they are dynamic. For static sources you may take a background spectrum and remove it.

Satellites: Past, Present, Future - by Dr. Katelynn Greer (LASP/CU Boulder)

Q: Why 6 satellites for GDC mission? What will be the altitude range for GDC observations?

A: Technically, the exact number of satellites has not yet been determined. However, a document called "Geospace Dynamics Constellation Design Reference Mission: Predicted Ephemeris Description" has been published which outlines a 6 satellite constellation mission. The expected altitude range for the in-situ measurements is discussed in detail in this document (Figure 6), but is approximately 350 – 400 km.

Q: When processing satellite data and deriving local parameters above a given Lat x Lon, is there a good rule of thumb for how wide a range of reported latitude and longitudes you should look over (as in averaging x-many degrees North-South East-West of the desired location)?

A: This really depends on the mission, the instrument, the viewing geometry, and the quantity being studied. Different missions have different orbits, and will have differing integrations periods or sampling areas. Different instruments will have differing resolutions. The viewing geometry could be nadir, off-nadir, or even limb viewing, all of which affects the latitude/longitude assigned to an observation. Lastly, you need to consider the quantity being observed: does it have large gradients over short spatial scales? Or temporal scales? All of these factors will determine how you can use the data over a given location or averaging.

Hierarchy of Atmospheric Modeling - by Dr. Xian Lu (Clemson Univ.)

Q: What is the typical delta_t for different atmospheric models?

A: It depends on the running models. For instance, if TIEGCM is running with two resolutions, then the delta_t will have to depend on the individual resolutions, such as if the horizontal resolution decreases then the delta_t will also decrease.

Q: Are the errors due to the numerics and the discretization quantified/estimated in numerical models?

A: Yes, the errors are due to numerical. Which can be eliminated by stopping at the second-order derivatives, and not enhancing towards higher-order derivatives.

Ion-Neutral Coupling - by Dr. Toshi Nisimura (Boston Univ.)

Q: Can the interaction between ions and neutral winds create heavier elements that can increase the overall mass of the plasma in movement? How would the energy transfer be in that case?

A: Good question. Yes, ion-neutral interaction changes the mass distribution. Vertical transport by heating brings molecular ions and neutrals from lower altitudes. Horizontal transport brings ions and neutrals from other regions that have different composition. The degree of the ion-neutral coupling will then change because of the modified composition. It's an active two-way coupling.

Q: How do you measure neutral winds?

A: There are two commonly used methods: 1) Fabry-Perot Interferometer. Doppler shift of an emission line gives the neutral wind speed. 2) Accelerometer on a low-Earth orbiting satellite. Satellite acceleration/deceleration can be used to deduce the wind speed.

Q: How important is it to study the neutral ion coupling at the low latitudes vs high latitudes?

A: Ion-neutral coupling is important at all latitudes. Because magnetospheric forcing is weaker at low latitudes, waves from the lower atmosphere have more impacts at low latitudes. Disturbance dynamo due to wind coming from high to low latitudes is another important thing.

Q: Can ion drag affect the neutral wind at lower latitude? if so what's the significance at different height?

A: Yes, ion drag is important at low latitudes. I only had time to cover a small set of examples, but there are many other examples at low latitudes as other speakers have presented. There are more examples like solar tides crating quiet time plasma drift and current system, and interhemispheric wind dragging ions across the equator. Ion drag is indeed height dependent because the wind speed and neutral-ion collision frequency vary with height.

Q: In your opinion, what observational capability are we lacking the most in terms of measuring ion-neutral collision frequency or other coupling mechanisms?

A: Good question. Ion-neutral composition is always a big problem. A good number of instruments provide density, velocity and temperature, but we have very limited capability of knowing what species of ions and neutrals are there. Ion-neutral coupling is highly dependent on the composition because the composition changes the chemistry and collision frequency.

Another important issue is structures across scales. We have reasonable understanding of global pictures, but it is very hard to resolve meso-scale (10s-100s of km horizontal) and small-scale (<10s of km to kinetic scale) structures.

Q: Normally MLT region is very dynamical and has varieties of energy sources, how could we tell whether the neutral is affected by the ions or something else? Is the magnitude of the ions energy competitive compared to other energy inputs?

A: We can only identify the cause-and-effect relation when the driving condition is well-defined. Ions quickly respond to magnetosphere energy input in ~min. Neutrals respond much more slowly (>10s of min). The time delay of observed ion and wind responds can indicate which one has responded first.

We also carry out simulations so that we can control the input and analyze force terms. Force terms can tell which one drives which. The relative importance of energy (and force) terms largely varies event-by-event. e.g., ion drag is usually important, but pressure gradient and other forces can become more important when the velocity is small or strong heating occurs.

Joule Heating - by Dr. Lindsay Goodwin, NJIT (5:14:09)

Q: What is the typical method joule heating is measured?

A: Great question! To "measure" the local Joule heating you need to measure all the parameters associated with it, such as the relative drift between ions and neutrals, the ion and neutral masses, and so on. Spacecraft and coupled observations from instruments like incoherent scatter radars and Fabry-Perot interferometers are all helpful for this. However, things become complicated if you want to examine the energy input and Joule heating globally or within a very large region (or with respect to altitude), due to data gaps. At that point, you would need to rely more on models.
However, calculating Joule heating can still be tricky, because there are values in the ionosphere that we still do not know, such as the ion-neutral collision frequency between O+ and O.

Q: How do the heat exchange rate compete with the frictional heating? Is this a valid thought?

A: That is a cool question! What I would say is you may recall my slide 8 equations, where I showed both the heat exchange rate between ions and neutrals:

$$Q_{EX} = \sum_i \frac{\rho_i \nu_{in}}{m_n + m_i} 3k_B(T_i - T_n)$$

and the frictional heating rate between ion and neutrals:

$$Q_F = \sum_i \frac{\rho_i \nu_{in}}{m_n + m_i} m_i(\mathbf{V_i} - \mathbf{V_n})^2$$

Certainly if you have a large temperature difference between ions and neutral, Ti-Tn, but a negligible relative drift between ions and neutrals, **Vi-Vn**, the heat exchange rate will be greater than the frictional heating rate. BUT you will notice that because **Vi-Vn** is squared, even a small relative drift between ions and neutrals can have a large impact, so we typically think of the frictional heating rate being "stronger" than the heat exchange rate.

Sudden Stratospheric Warming - by Dr. Nick Pedatella, HAO/NCAR

Q: Does the enhancement in lunar tide has any effect on the enhancement of migrating semidiurnal tides?

A: It is unlikely that the enhanced lunar tide influences the migrating semidiurnal tides during SSWs. However, there is no existing research that I am aware of that has investigated this question specifically.

Q: Is there any delay in response at the equatorial latitude from when the SSW occurs at higher latitude?

A: There are typically a few days delay between the onset of the SSW (defined as the reversal of the zonal mean zonal winds at 60° N and 10 hPa) and the strongest response in the equatorial region. Note that the timing of the strongest response in the equatorial region relative to the SSW depends partly on the definition of the SSW onset.

Q: how do we tell the causality between SSWs and the enhanced PW activities?

A: Early investigations into the formation of SSWs using relatively simple models demonstrated that the interactions of planetary waves with the zonal mean flow leads to the formation of SSWs. See, for example, Matsuno (1971, doi:10.1175/1520-0469(1971)028<1479:ADMOTS>2.0.CO;2).

Acoustic Waves - by Dr. Pavel Inchin, Embry-Riddle Aeronautical Univ. (5:44:27)

Q: Why does the speed of sound increase in the stratosphere and thermosphere?

A: Considering the atmosphere as an ideal gas (sufficient approximation for many problems), we find that the speed of sound is directly proportional to its temperature and composition ($c=\sqrt{(\gamma RT/M)}$, where c – speed of sound, γ – gas constant, R – specific gas constant, M – molecular mass and T - temperature). Thus, the increase of temperature in the stratosphere, driven by the heat from the formation of ozone, leads to the increase of speed of sound in this region. Likewise, the increase of temperature from sun light absorption (along with the change of composition from diatomic to dominantly monoatomic gas) leads to the increase of speed of sound in the thermosphere.

Original talks are available at:

https://www.youtube.com/watch?v=uUrx5FdJlnY

Textbook resources for CEDAR Science:

http://cedarweb.vsp.ucar.edu/wiki/images/f/f1/2020CEDAR_Knipp_Book_shelf_titles.pdf

CEDAR 2021 - STUDENT NEWSLETTER

Designed by Fan Yang
Reviewed by Dr. Komal Kumari, Dr. Astrid Maute, Zishun Qiao, and Dr. Larisa Goncharenko

Sponsored by
The National Science Foundation

#FROMSTUDENTSFORSTUDENTS

Photo credit: canva.com